

CHAPTER-3

Study of inhibition of copper corrosion in alkaline medium by azoles:

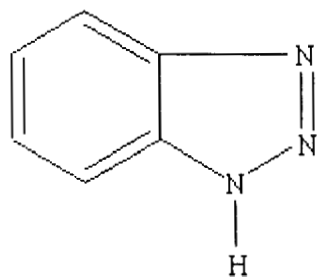
3.0 Introduction:

The corrosion inhibitors of copper are generally heterocyclic compounds containing nitrogen and sulphur [1]. From the literature we find that several azole compounds have been used as inhibitors and detailed studies carried out on some of them from the point of view of their inhibitor efficiency. Recent attention has been paid to compounds such as Benzotriazole, Mercaptobenzothiazole etc. as corrosion inhibitors [2-5]. In this chapter we discuss the results obtained in studying azoles as inhibitors of copper corrosion in 0.1 N NaOH solution. The analysis of the inhibiting properties of these compounds has been carried out by cyclic voltammetry (CV) and electrochemical impedance measurement. The influence exerted by concentration on their inhibiting efficiency has also been considered.

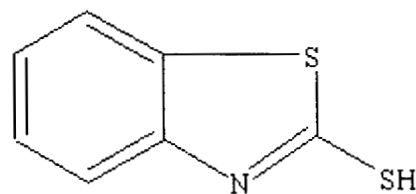
The different azoles studied were *Benzotriazole* (BTA), *Mercaptobenzothiazole* (MBT), *Benzimidazole* (BIMD), *Mercaptobenzimidazole* (MBIMD), *Imidazole* (IMD) and *Tetrazole* (TTA). All these azoles have nitrogen or sulphur or both groups present in the molecule.

3.1 Structure:

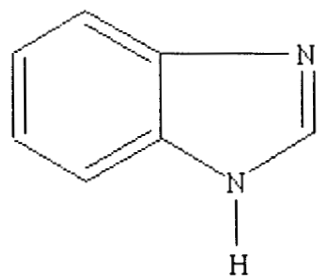
The structures of the azoles are as follows:



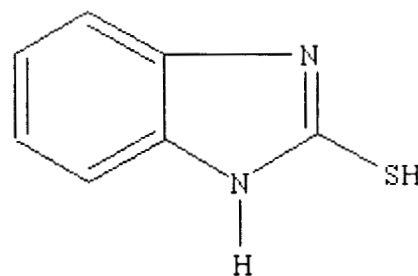
Benzotriazole (BTA)



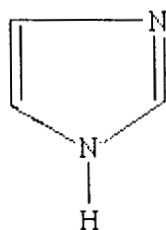
Mercaptobenzothiazole (MBT)



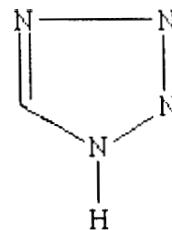
Benzimidazole (BIMD)



Mercaptobenzimidazole (MBIMD)



Imidazole (IMD)



Tetrazole (TTA)

A study of the relative corrosion inhibition efficiency of these molecules on copper has been undertaken in this work. The structural similarity of these molecules makes such a study quite interesting. This also helps to identify the primary causes of their inhibition action. The relative inhibition efficiencies are measured by the cyclic voltammetric method of measuring the charge involved in surface redox reaction in alkaline media as described in the chapter. Once the charge involved in the reaction is measured, the inhibition efficiency is calculated from the formula,

$$I = \left(1 - \frac{Q_{in}}{Q_{bl}} \right) \times 100 \quad (1)$$

where , I is the Inhibition efficiency

Q_{in} is the charge in the presence of inhibitor

Q_{bl} is the charge in the absence of the inhibitor.

The charge is obtained by integrating the area under the $I - V$ curve of the cyclic voltammogram.

3.2 Surface coverage:

The extent of adsorption is usually expressed as a surface coverage θ i.e. the fraction of the surface covered by the adsorbate. Adsorption can be considered as a competition between all species in the system for sites on the electrode surface. Hence θ will depend on the solvent, electrolyte, adsorbate structure, concentration and the concentration of any other species in the system as well as on the nature of the electrode. An adsorption isotherm gives the relationship between the coverage of an interface with an adsorbed species and the concentration of the species in the solution. Various adsorption isotherms have been formulated. Interpretation of adsorption type, organic inhibitor performance data can be obtained by fitting the

data to one of the adsorption isotherms. From the plot the equilibrium constant and free energy of adsorption of the organic inhibitor can be measured.

We have calculated the surface coverage of the electrode surface θ as,

$$\theta = 1 - \frac{Q_{in}}{Q_{bl}} \quad (2)$$

This method of calculating the surface coverage by measurement of charge under the cyclic voltammetric peaks has been used by Babic et al [6]. They have calculated the surface coverage of BTA on copper at different concentrations in 1M Sodium acetate solution.

The different types of adsorption isotherms are as follows: [7]

$$1. \text{ Henry} \quad kc = RT\theta \quad (3)$$

$$2. \text{ Freundlich} \quad kc^n = \theta \quad (4)$$

$$3. \text{ Langmuir} \quad kc = \frac{e}{1-e} \quad (5)$$

$$4. \text{ Frumkin} \quad kc = \frac{e}{1-\theta} \exp(-2a\theta) \quad (6)$$

$$5. \text{ Parsons} \quad kc = \frac{\theta}{1-\theta} \exp\left[\frac{2-\theta}{(1-\theta)^2}\right] \exp(-2a\theta) \quad (7)$$

$$6. \text{ Blomgren and Bockris} \quad kc = \frac{\theta}{1-\theta} \exp(a_1\theta^{1/2} - a_2\theta^3) \quad (8)$$

$$7. \text{ Helfand - Frisch - Lebowitz} \quad kc = \frac{\theta}{1-\theta} \exp\left[\frac{2-\theta}{(1-e)}\right] \quad (9)$$

where c is the concentration of the ions, a is the interaction parameter, θ is the fractional surface coverage. k is the adsorption equilibrium constant.

The relation between the adsorption equilibrium constant k and the free energy of adsorption ΔG is given by the expression,

$$k = \frac{1}{c_{\text{solvent}}} \exp\left(\frac{-\Delta G}{RT}\right) \quad (10)$$

where c_{solvent} is the molar concentration of the solvent which in the case of water is 55.5 moles litre⁻¹.

3.3 Experimental:

3.3.1 Cyclic voltammetry:

A conventional three electrode cell was used for cyclic voltammetric studies. The counter electrode was a platinum strip of approximately 2 cm² surface area. All the potentials were measured against *Hg/Hg₂SO₄/sat. Na₂SO₄* reference electrode. The stability of its potential has been verified by keeping in the medium of study for 24 hours and measuring its potential. All the experiments were conducted in an atmosphere of oxygen free nitrogen gas. The electrolyte was 0.1N NaOH prepared in millipore water. Cyclic voltammetry (CV) was carried out using an EG&G potentiostat (Model 263A) interfaced to a PC through a GPIB card (National Instruments). Charge measurements were carried out from the first scan CV in each case. The scan rate was fixed at 20 mVsec⁻¹. For copper the potential range was fixed between -1.5 V to -0.2 V. CV readings were taken after 30 minutes of dipping the copper electrode into the solution containing inhibitor for all concentrations studied.

3.3.2 Electrochemical impedance spectroscopy:

Electrochemical impedance spectroscopy was performed using an EG&G potentiostat (Model 263A) along with a lock in amplifier (Stanford Research Systems Model SR830). A pure sine wave of 4mV amplitude was derived from the lock- in amplifier for application to the cell. The current output was in turn

connected to the lock-in amplifier input. Impedance was measured over a frequency range of 1Hz to 30kHz. All the impedance experiments were carried out 30 minutes after dipping the working electrode into 0.1N NaOH solution containing the inhibitor at the rest potential (-600mV). The concentration of the inhibitors used was 1mM in all the cases.

For cyclic voltammetric and electrochemical impedance measurements, copper specimen of purity $>99.9\%$ was used in the form of metal strips. A well defined region of the electrode was exposed to the electrolyte, the remaining portion being well insulated with Parafilm and teflon. The geometric area of the electrode exposed to the electrolyte was 0.8 cm^2 . The metal surface was hand polished with emery papers of grades 800,1000,1500 (3M make) whose particle sizes are $17\mu\text{m}$, $13\mu\text{m}$ and $9\mu\text{m}$ respectively. The electrode after polishing was rinsed in distilled water. It was then polished successively on a microcloth having a slurry of 1,0.3,0.05 μm alumina powder (Buehler). After polishing, the electrode was sonicated in distilled water to remove the alumina particles and then immersed into the electrochemical cell.

3.3.3 Inhibitors:

The different inhibitors studied were Benzotriazole (BTA), Mercaptobenzothiazole (MBT), Benzimidazole (BIMD), Mercaptobenzimidazole (MBIMD), Imidazole (IMD) and Tetrazole (TTA).

3.4 Cyclic voltammetric Results:

The cyclic voltammogram of bare copper electrode polished with $0.05\mu\text{m}$ alumina particles in 0.1N NaOH is shown in figure 1. The CV was taken after 15 minutes of immersion and at room temperature. The cyclic voltammogram of copper in 0.1N NaOH solution shows three anodic and two cathodic peaks. The first anodic peak corresponds to the oxidation of Cu to Cu_2O monolayer formation. The

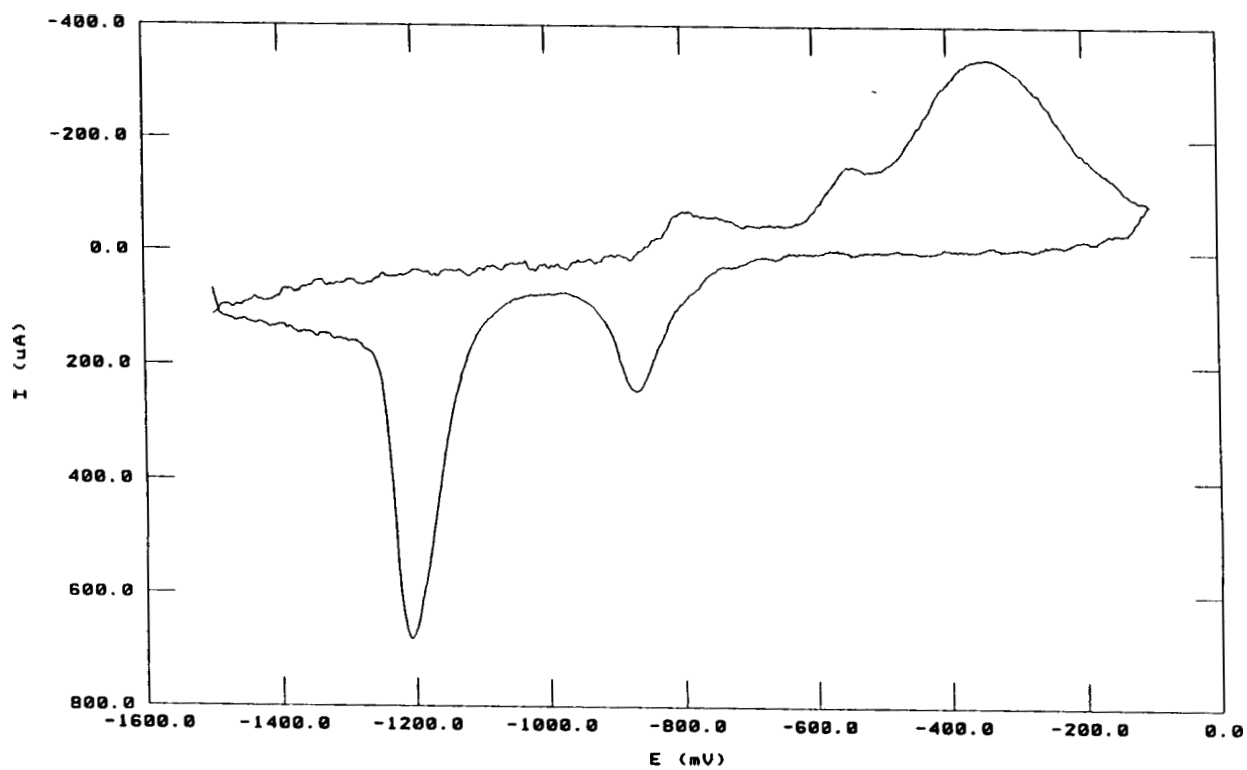


**Fig 1: CV of copper in 0.1 N NaOH. Scan rate : 20 mV sec^{-1}
Potential is referred with respect to $\text{Hg} / \text{Hg}_2\text{SO}_4$ (sat. Na_2SO_4)**

second and third peaks are ascribed to the multilayer formation of CuO in parallel pathways, viz. the oxidation of Cu₂O to CuO and another directly from Cu by two electron transfers [8]. In the reverse scan the fourth peak corresponds to the cathodic reduction of CuO to Cu₂O while the fifth one is due to the reduction of Cu₂O to Cu.

The electrochemical impedance spectrum of Cu in 0.1 N NaOH is shown in figure 2. The real and imaginary components of the impedance are plotted on the x and y axes respectively (Cole-Cole plot)(figure 2). The Cole-Cole plot shows both kinetically controlled (semi circular) and diffusion controlled (linear, unity slope) regions. By extrapolation of the kinetic region R_{ct} and C_{dl} can be measured (figure 3). [9,10].

The R_{ct} and C_{dl} values are found to be $258\Omega cm^2$ and $13.7 \mu F cm^{-2}$ respectively.

3.4.1 Measurement of inhibition efficiency by cyclic voltammetry:

An inhibitor reduces the corrosion rate of an electrode by adsorbing on the electrode surface and reducing the corrosion current i_{corr} . As a consequence the charge transfer resistance increases. By sweeping the potential and measuring the charge required for anodic and cathodic reactions, it is possible to estimate the magnitude of the corrosion process electrochemically. Addition of inhibitor leads to a reduction of charge measured from the cyclic voltammetric curve. While in principle, one can measure charge either from anodic or cathodic curves, we have chosen the cathodic peaks for our charge measurement as they are generally very well defined and sharp.

Figures 4-9 shows the cyclic voltammetric curves of Cu in 0.1 M NaOH in the presence of BTA, MBT, BIMD, MBIMD, IMD and TTA at a concentration of 1 mM as compared to blank.

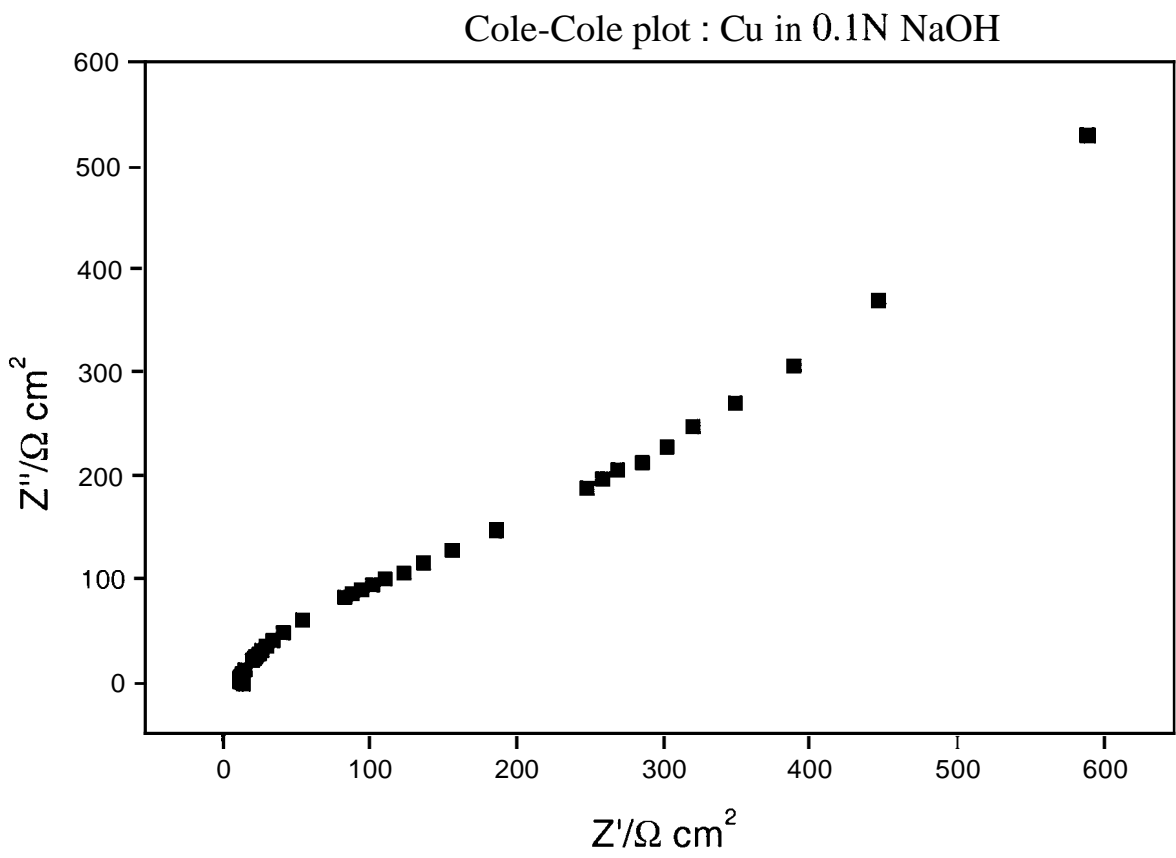
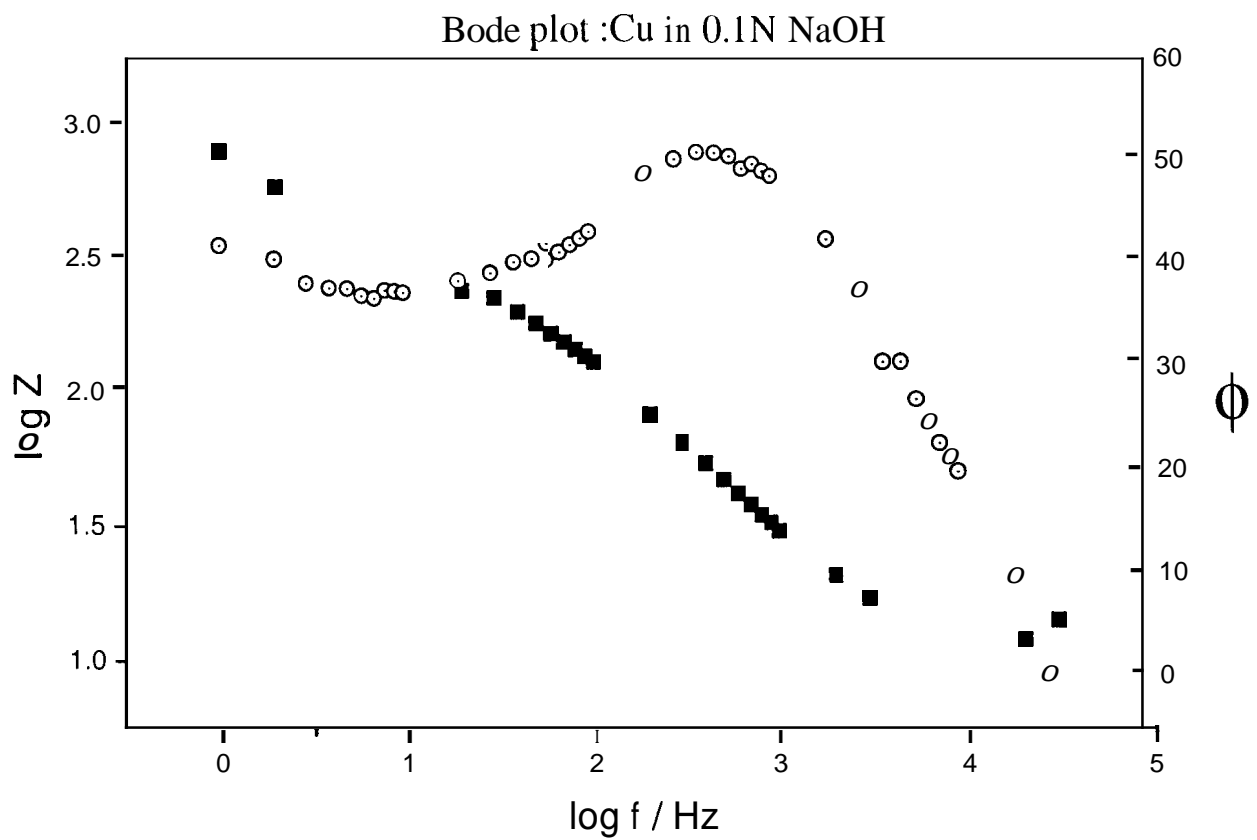


Figure - 2

Cole - Cole plot : Cu in 0.1N NaOH

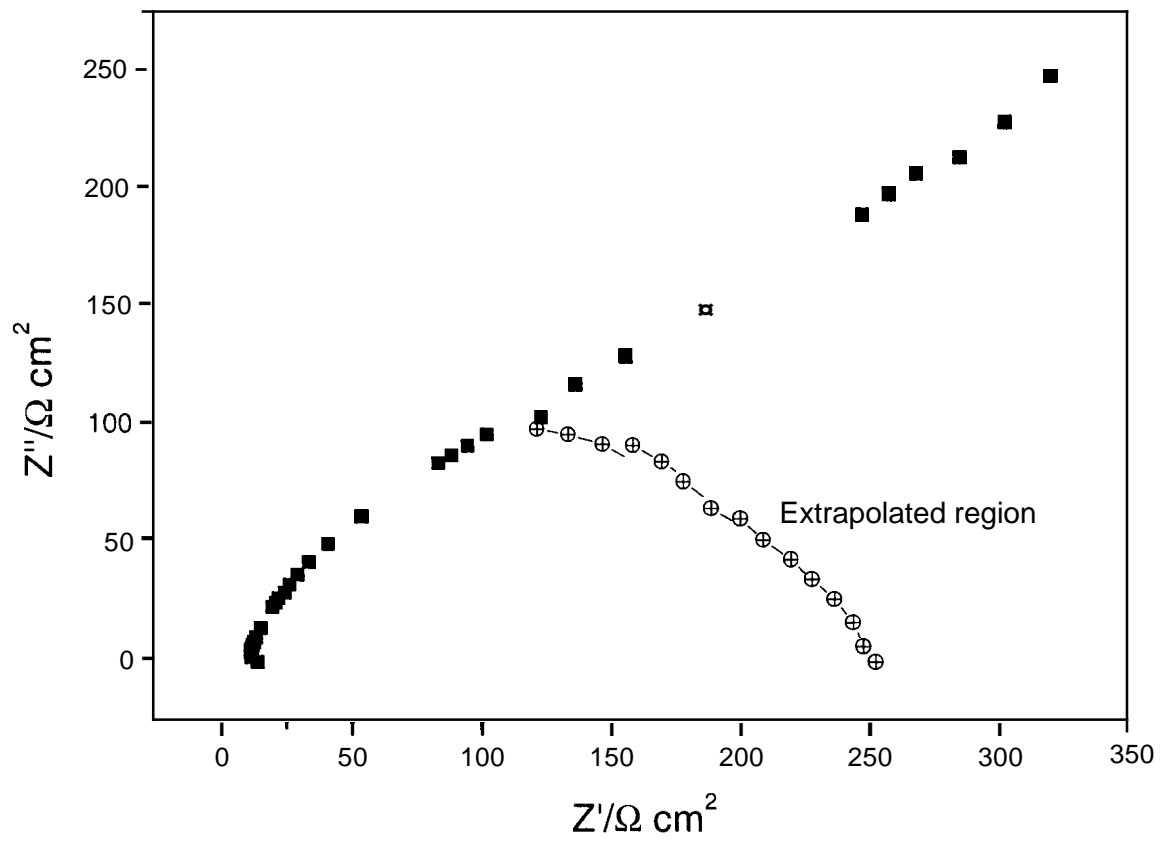


Figure - 3

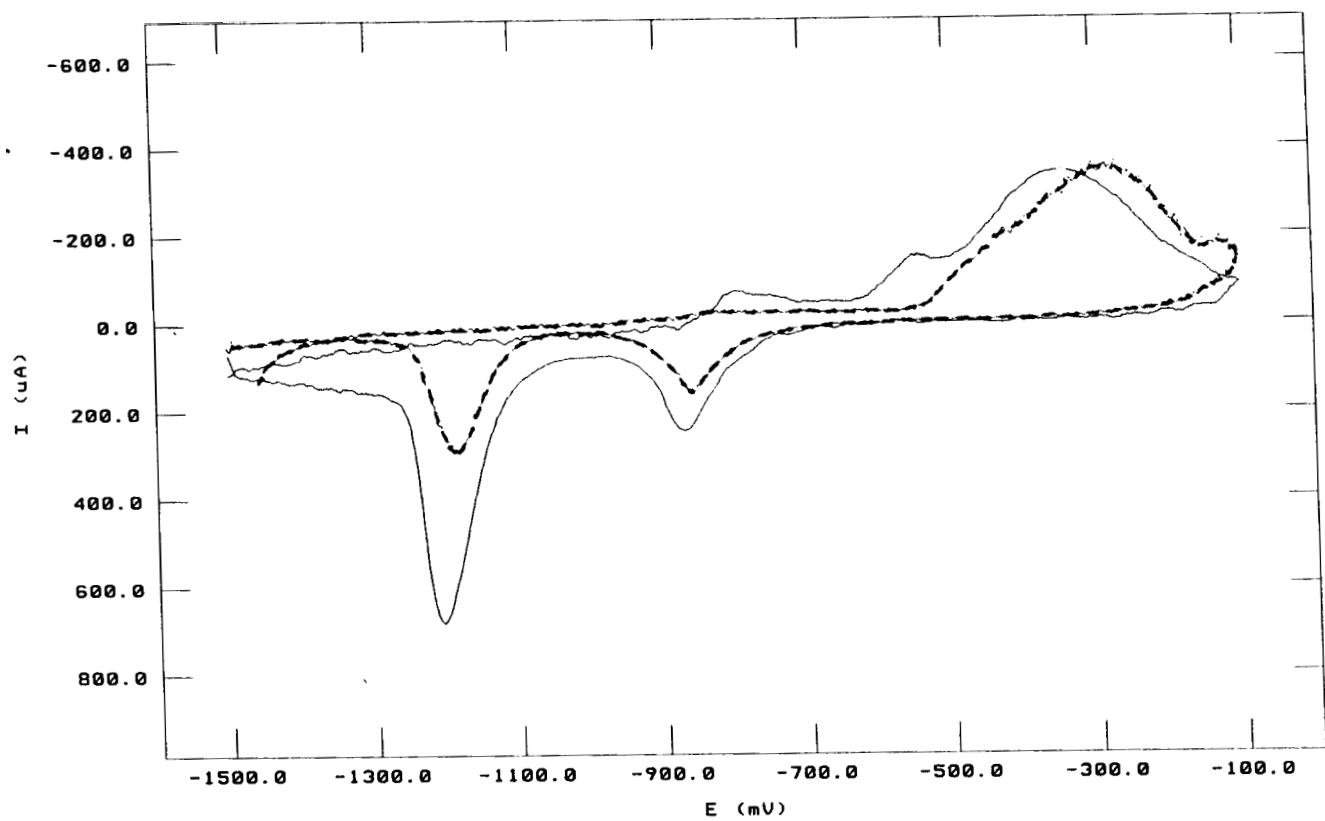


Fig 4 : CV of copper in 0.1N NaOH + 1mM Benzotriazole (BTA)

Scan rate : 20 mV/ s

————— Blank

- - - - - With BTA

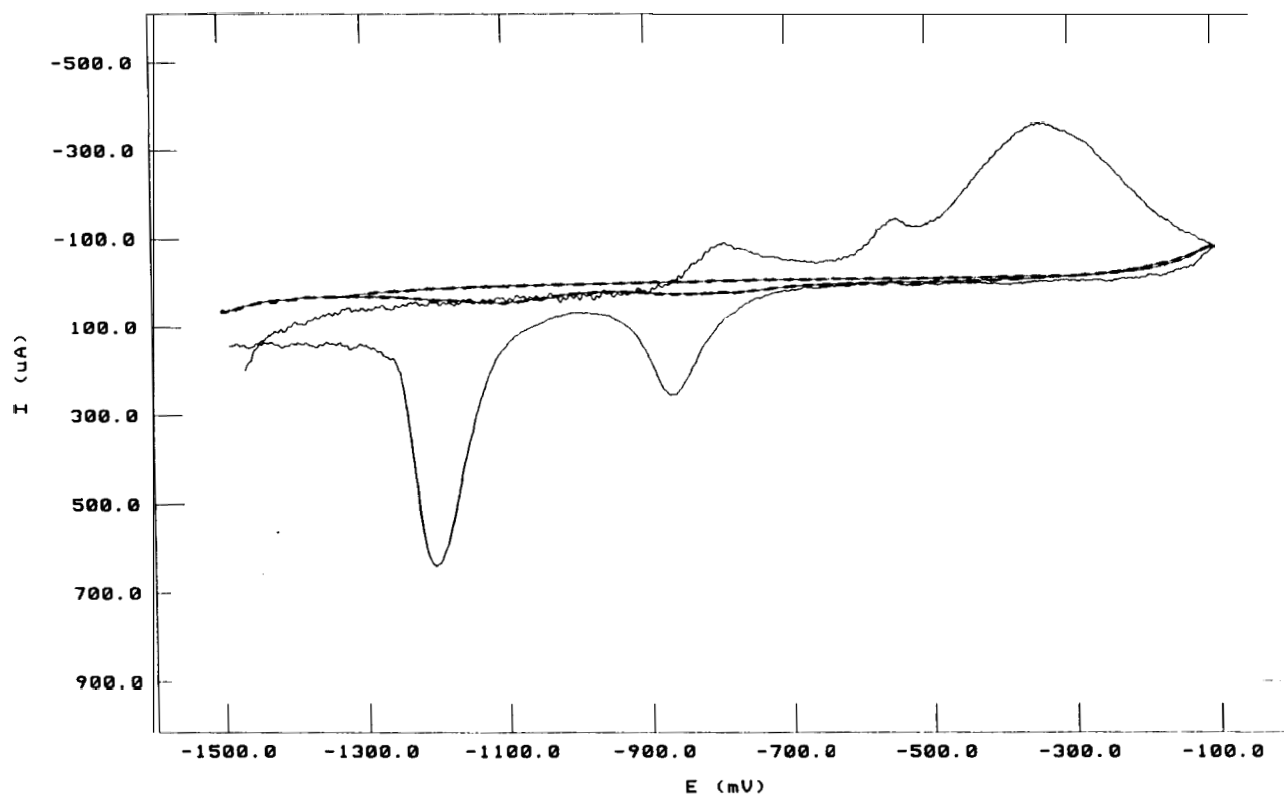


Fig 5 : CV of copper in 0.1N NaOH + 1mM Mercaptobenzothiazole (MBT)

Scan rate : 20 mV/s

———— Blank - - - - - With MBT

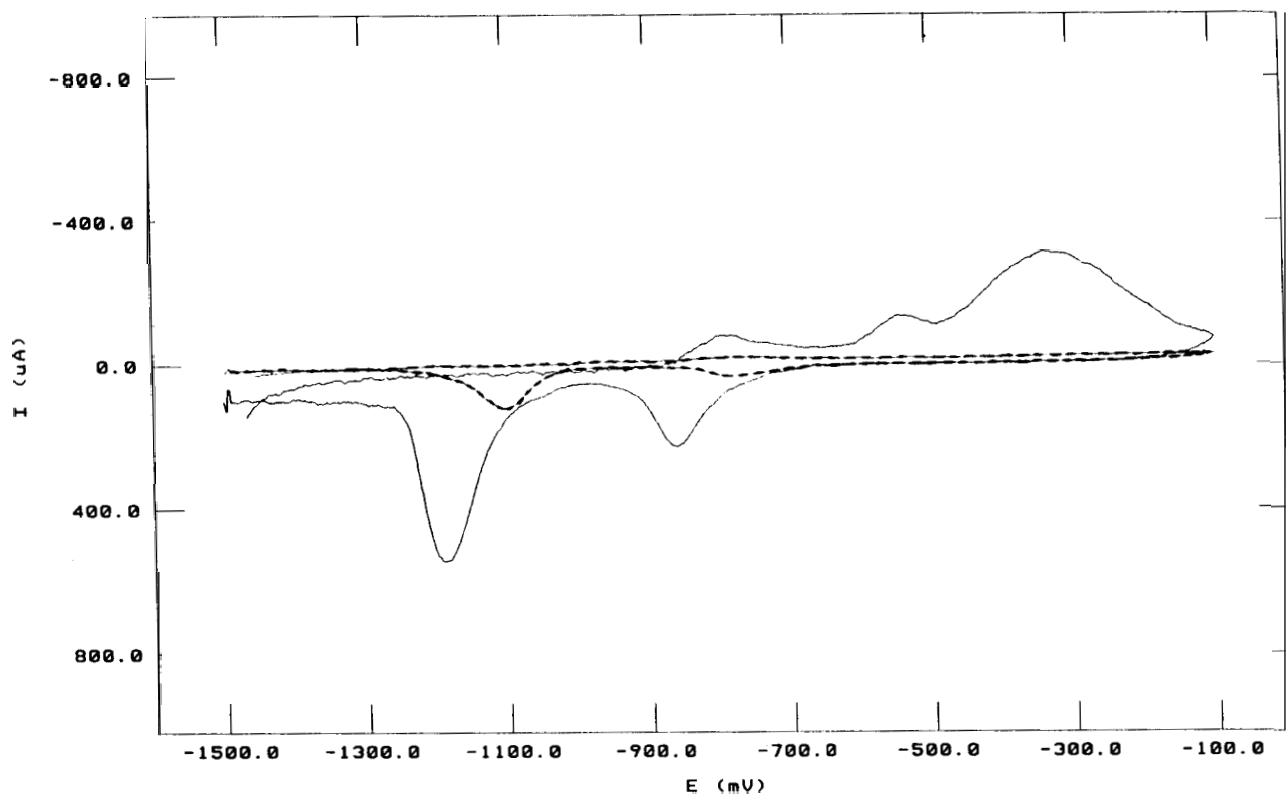


Fig 6 : CV of copper in 0.1N NaOH + 1mM Benzimidazole (BIMD)

Scan rate : 20 mV/ s

———— Blank - - - - - With BIMD

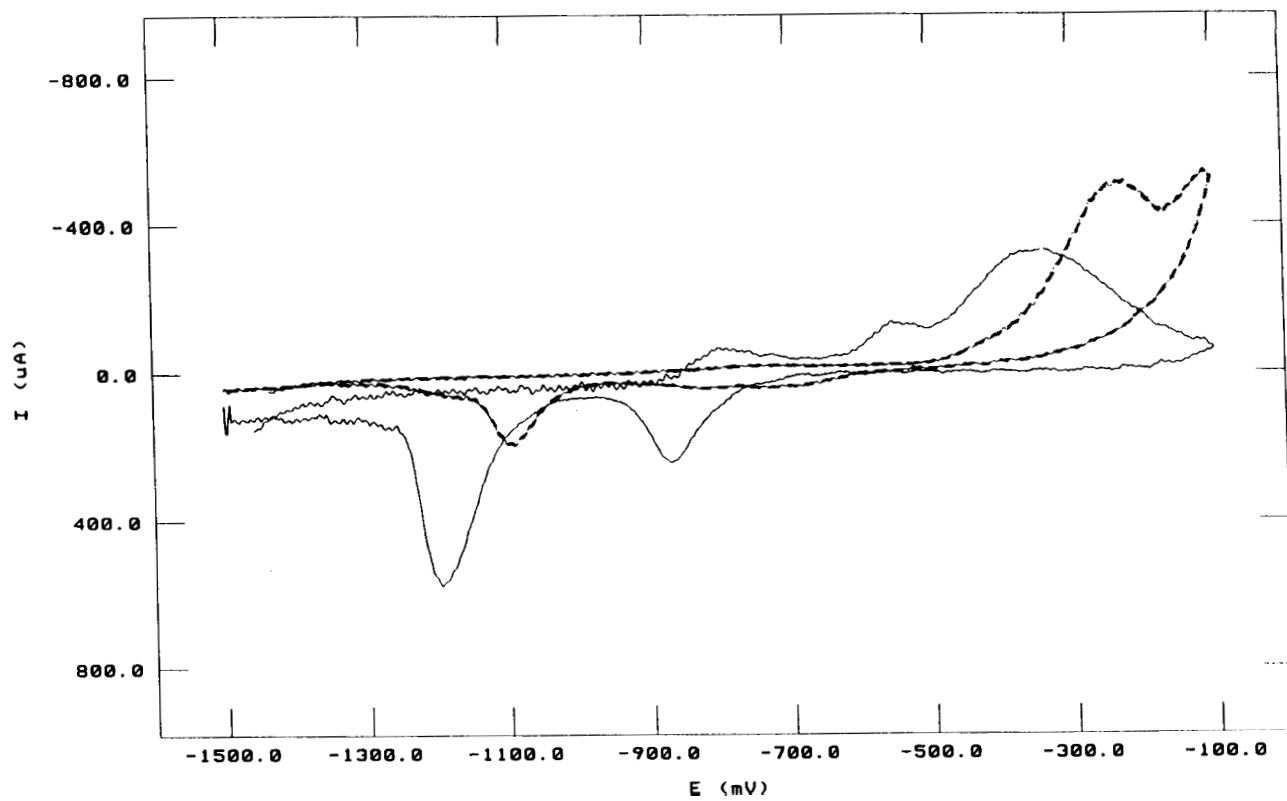


Fig 7 : CV of copper in 0.1N NaOH + 1mM Mercaptohenzimidazole (MBIMD)

Scan rate : 20 mV/s

————— Blank - - - - - With MBIMD

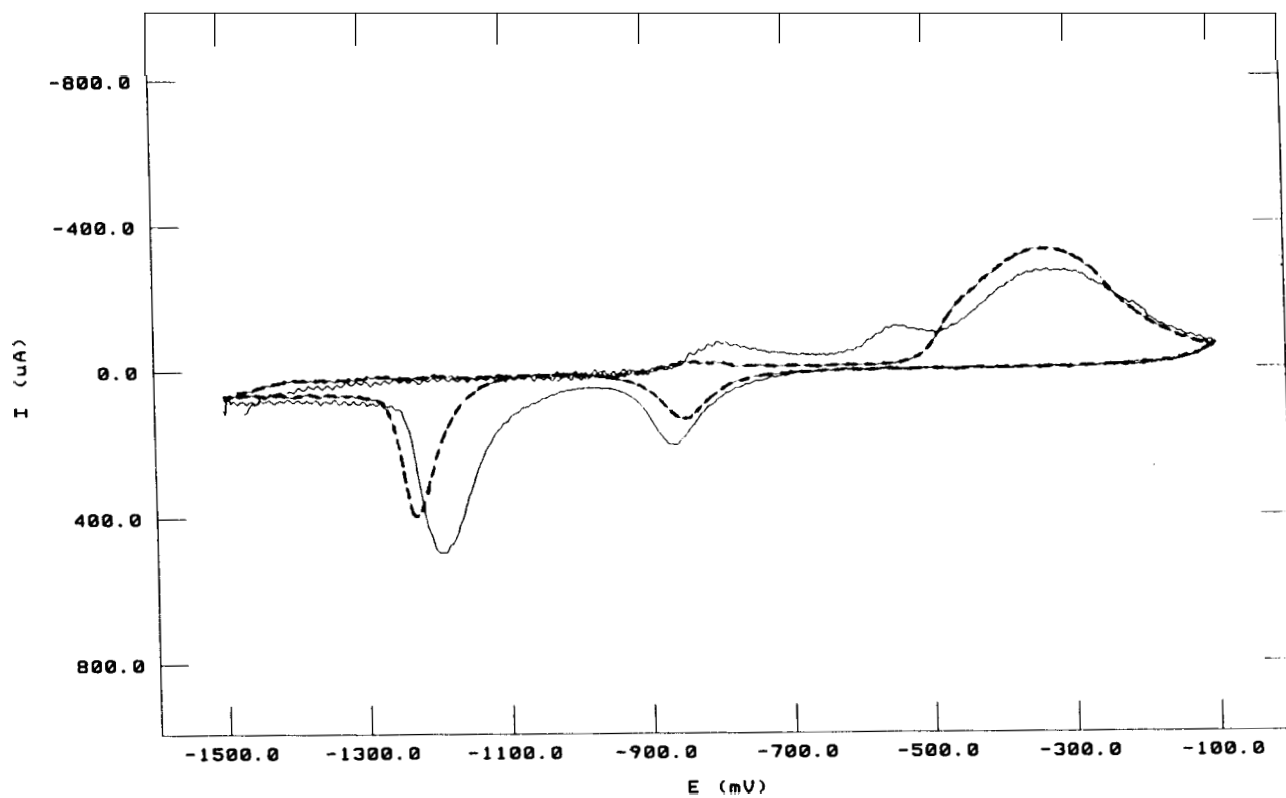


Fig 8 : CV of copper in 0.1N NaOH + 1mM Imidazole (IMD)

Scan rate : 20 mV/s

————— Blank

- - - - - With IMD

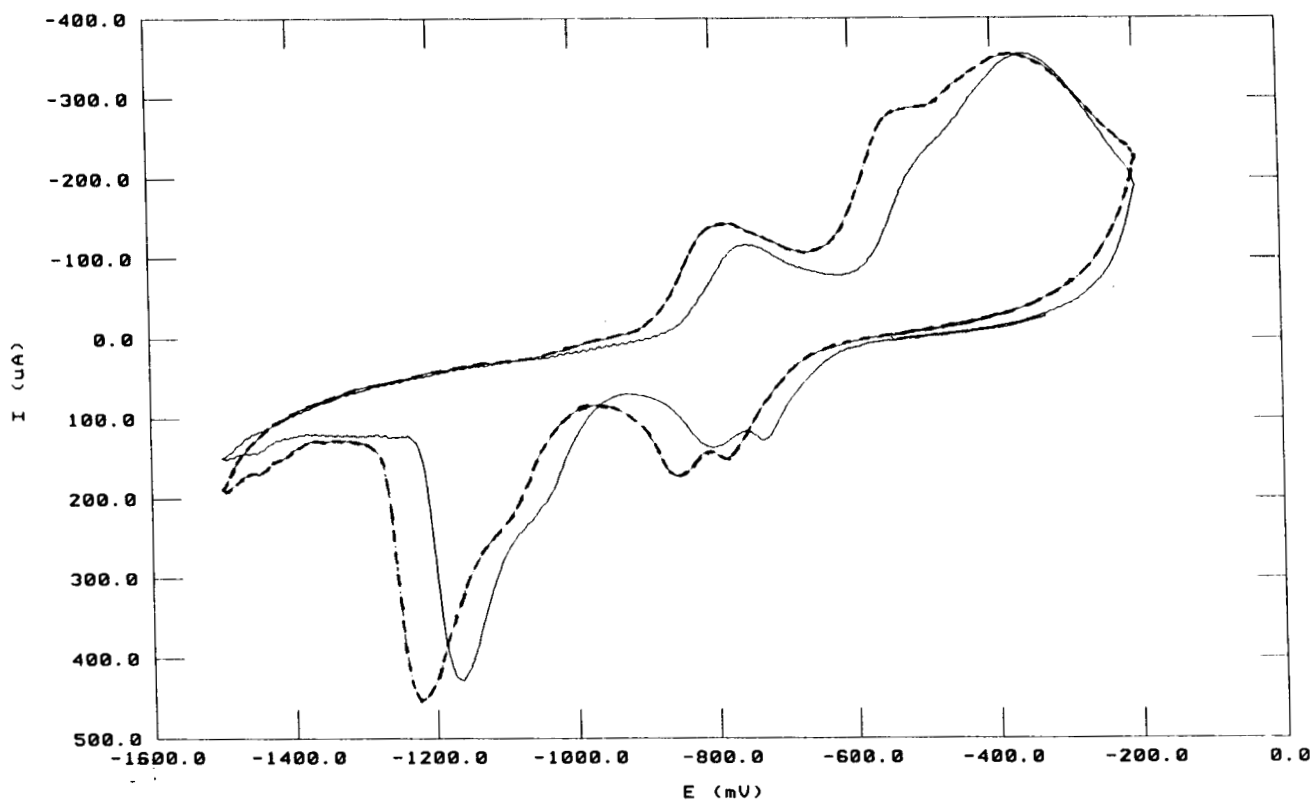


Fig 9 : CV of copper in 0.1N NaOH + 1mM Tetrazole (TTA)

Scan rate : 20 mV/s

———— Blank - - - - - With TTA

We find that as the concentration of the inhibitor increases the current and consequently the charge under the oxidation-reduction curves progressively reduces. At lower inhibitor concentrations the current though lower than the blank value does not affect the peak potential significantly. At higher inhibitor concentrations however there is a shift in peak potentials. The curves are also more drawn out. The values of measured charge during the cathodic scan at different concentrations and inhibitors are shown in Table 1

Table 1

Cathodic charge (mC cm^{-2}) for copper in 0.1M NaOH after the addition of different inhibitors at various concentrations (Blank value = 6.1 mC cm^{-2})

<i>Concentration (mM)</i>	<i>BTA</i>	<i>MBT</i>	<i>BIMD</i>	<i>MBIMD</i>	<i>IMD</i>
0.1	5.40	4.40	5.00	4.65	5.03
0.2	4.48	3.08	3.00	3.88	4.56
0.5	3.32	2.27	1.53	3.05	3.95
0.7	2.86	1.43	1.38	2.65	3.71
1.0	2.59	0.94	1.24	1.89	3.42
2.0	2.13	0.64	1.06	1.55	3.27

Among the azoles studied, Tetrazole (TTA) is not found to have any effect on the cyclic voltammetric peaks of Cu in 0.1M NaOH. Hence it is not expected to function as an inhibitor for the corrosion of Cu in 0.1M NaOH.

3.5 Impedance studies:

The impedance spectra of Cu in 0.1M NaOH in the presence of different azoles are shown in figures 10-14. The data is plotted in both Bode plot and Cole-Cole plot forms. We find that as the inhibitor gets adsorbed onto the electrode surface the charge transfer resistance R_{ct} increases. The double layer capacitance C_{dl} reduces after adsorption of the inhibitor since the adsorbed film acts as a dielectric between the metal and electrolyte. The large semi circles observed from high to low frequencies indicates that the charge transfer resistance becomes dominant in the corrosion process due to adsorption of the inhibitor.

For a typical Randles equivalent circuit a plot of Z' versus Z'' for various frequencies is a semicircle which cuts the real axis at high and low frequency ends. At high frequency cut off Z corresponds to uncompensated resistance R_s and at low frequency it is $R_s + R_{ct}$. From the impedance plots of inhibitor covered copper electrode we find that the semi circle in the Cole-Cole plot does not intersect the x-axis at low frequencies. The value of R_{ct} is obtained by extrapolation of the impedance plot at the low frequency region.

The double layer capacitance C_{dl} is determined from the corner frequency of the $\log Z$ vs. $\log f$ plot (Bode plot). The corner frequency at the high frequency end of the spectrum is given as,

$$f_h = \frac{1}{2\pi R_s C_{dl}}$$

R_s can be found out from the intersection of the extrapolated portion of the high frequency plateau on the y-axis. Thus knowing f_h and R_s , C_{dl} can be evaluated from the above expression.

The charge transfer resistance R_{ct} and the double layer capacitance C_{dl} values of Cu in 0.1 M NaOH in the presence of different azoles are shown in Table 2

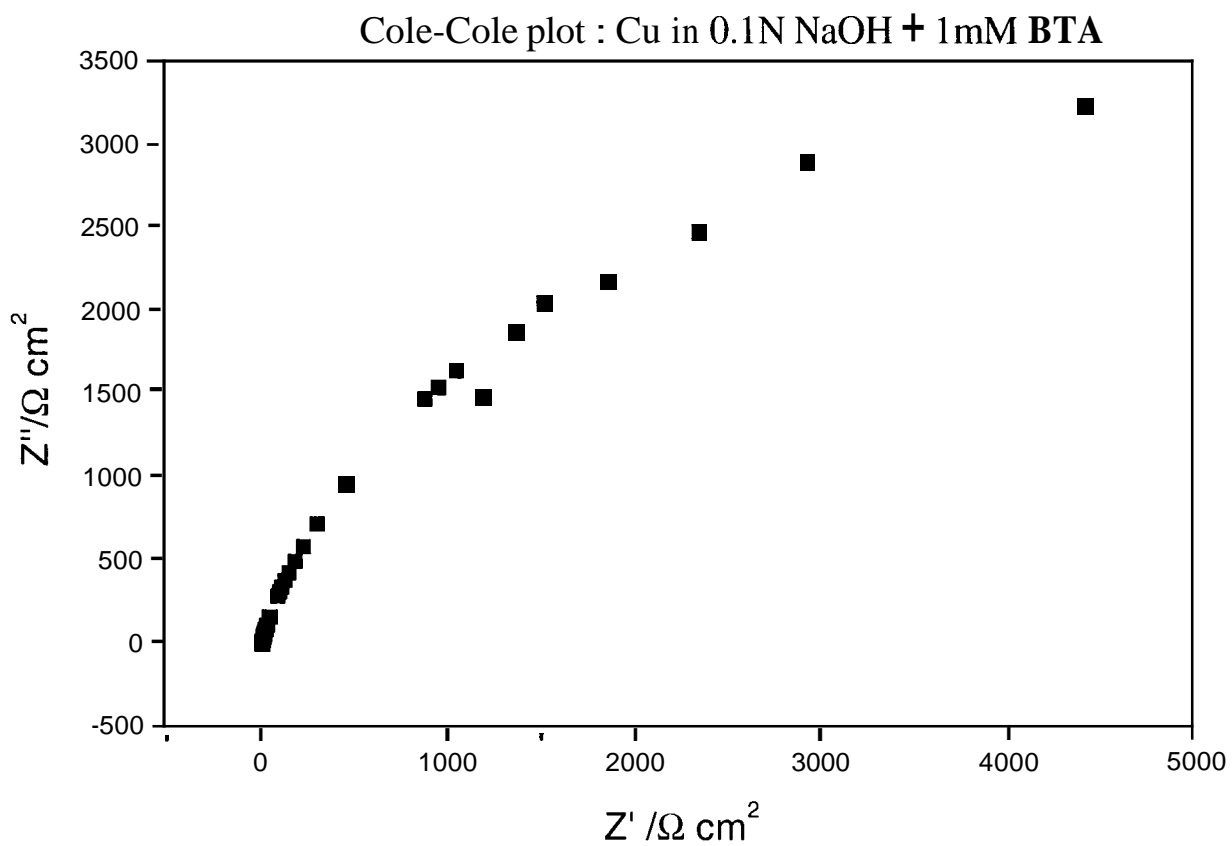
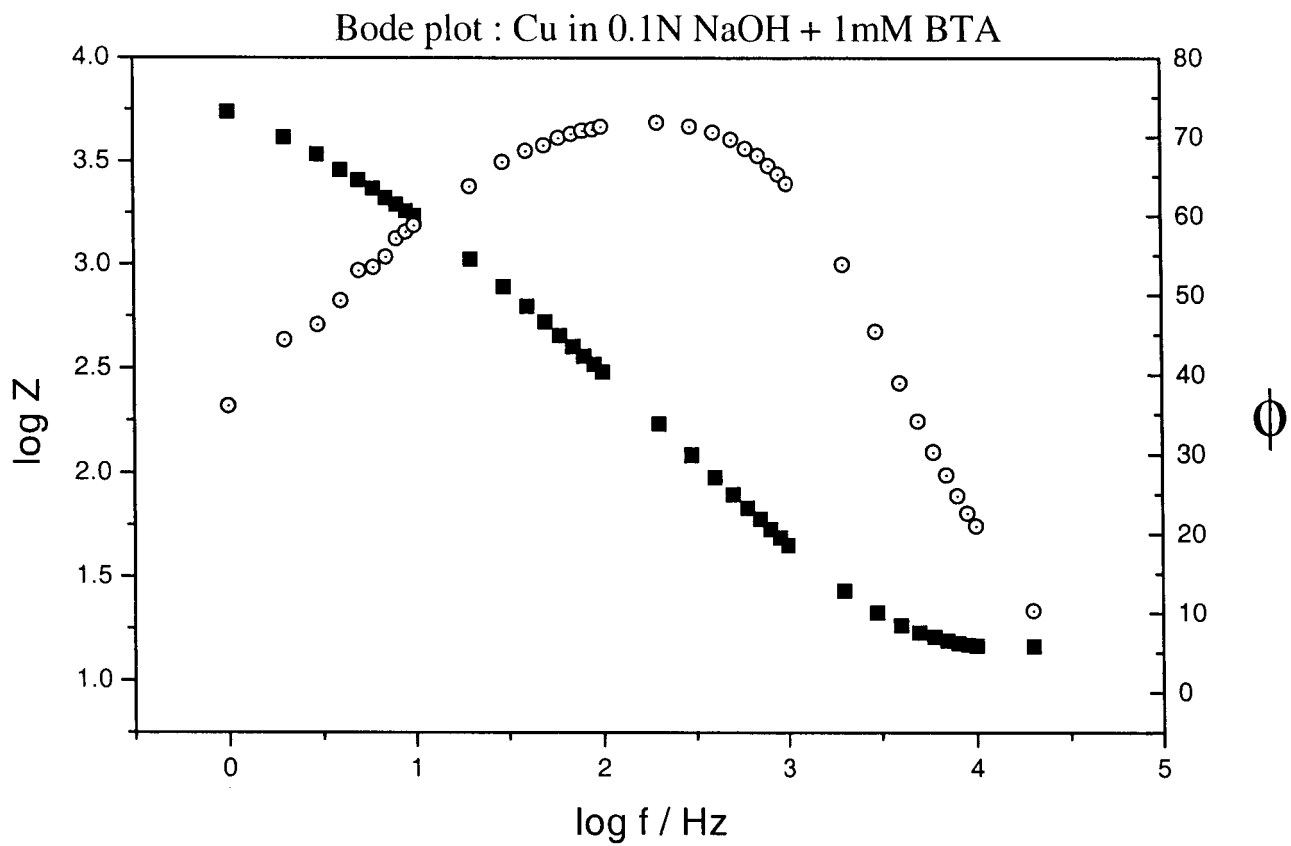


Figure - 10

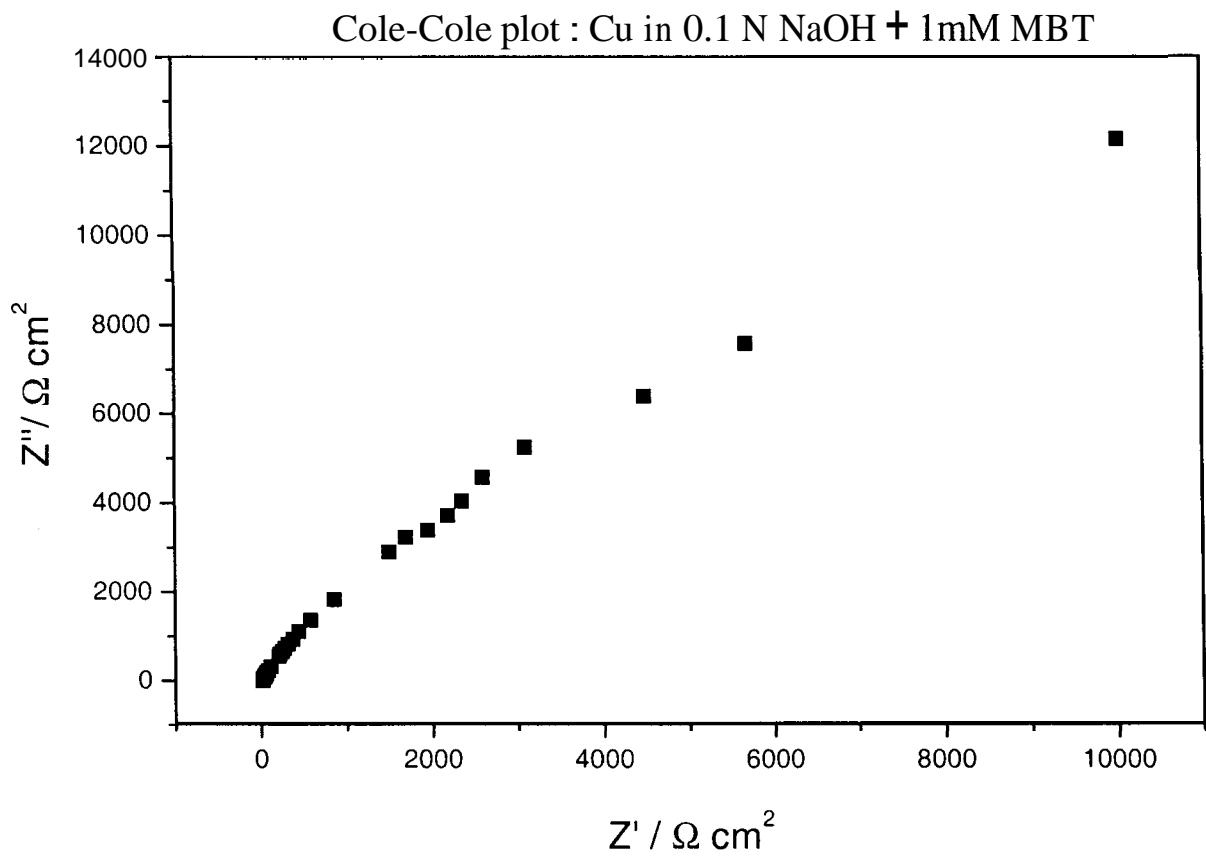
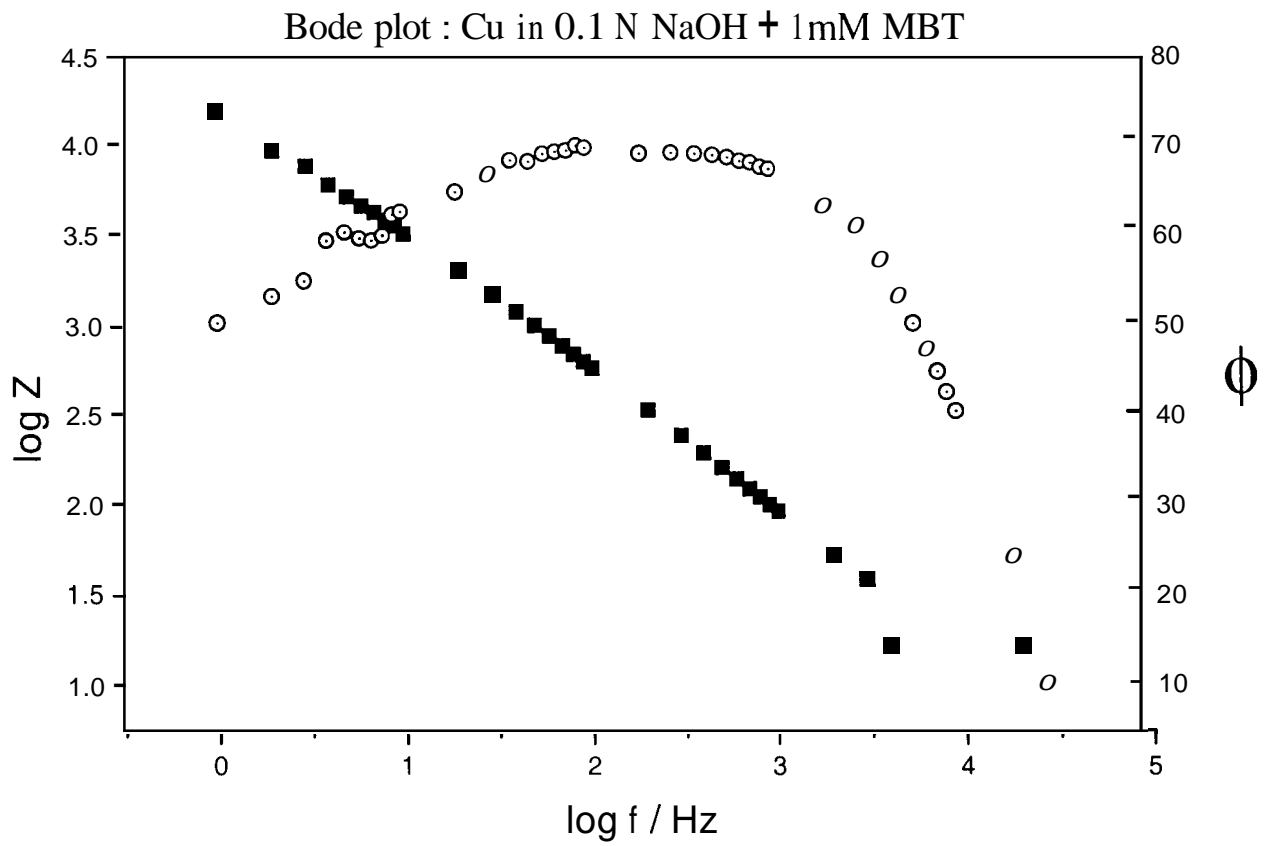


Figure - 11

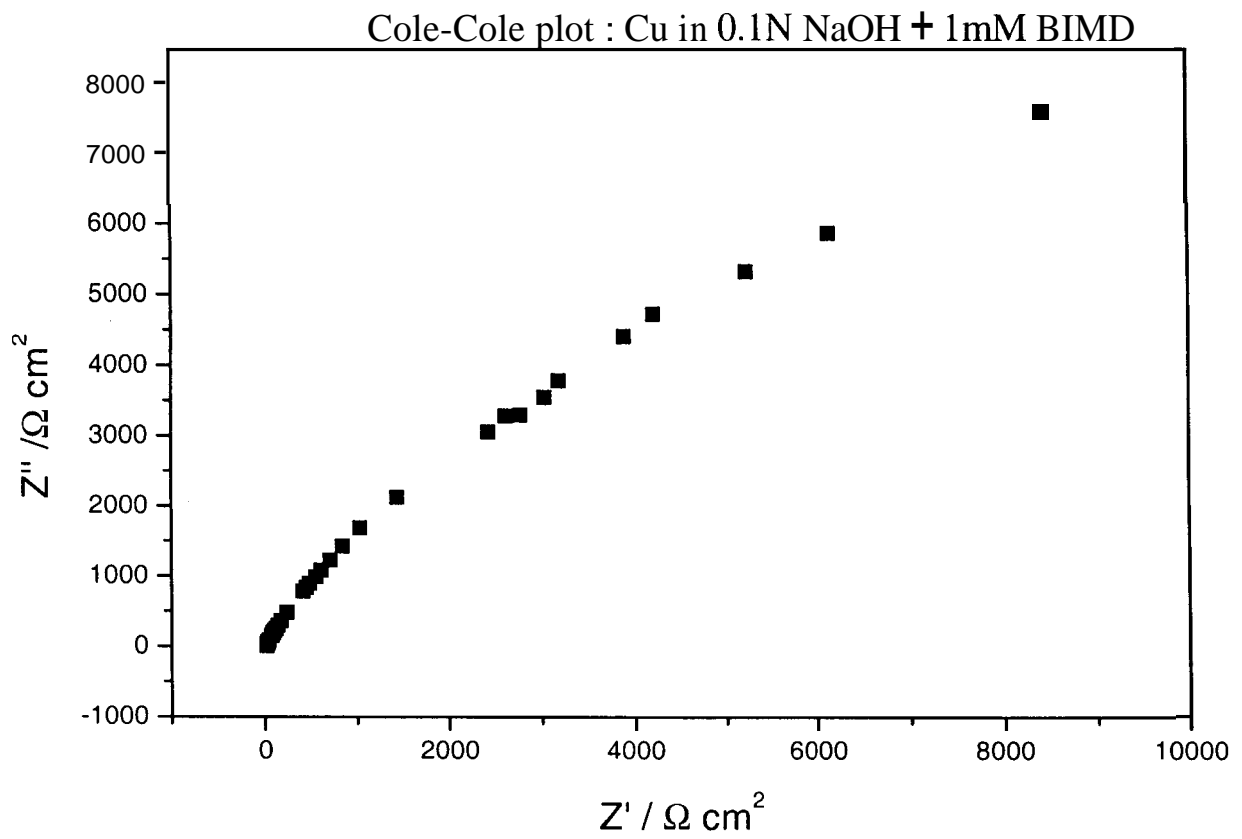
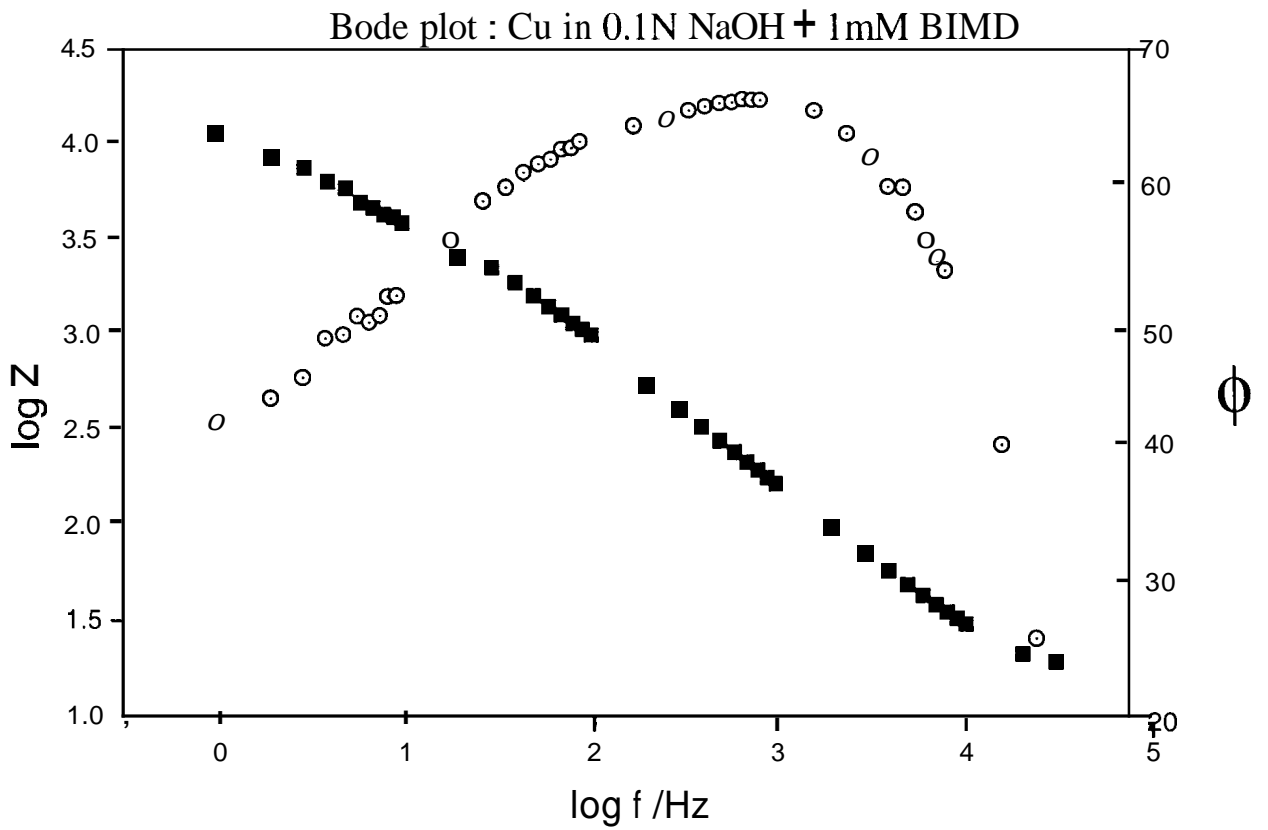


Figure - 12

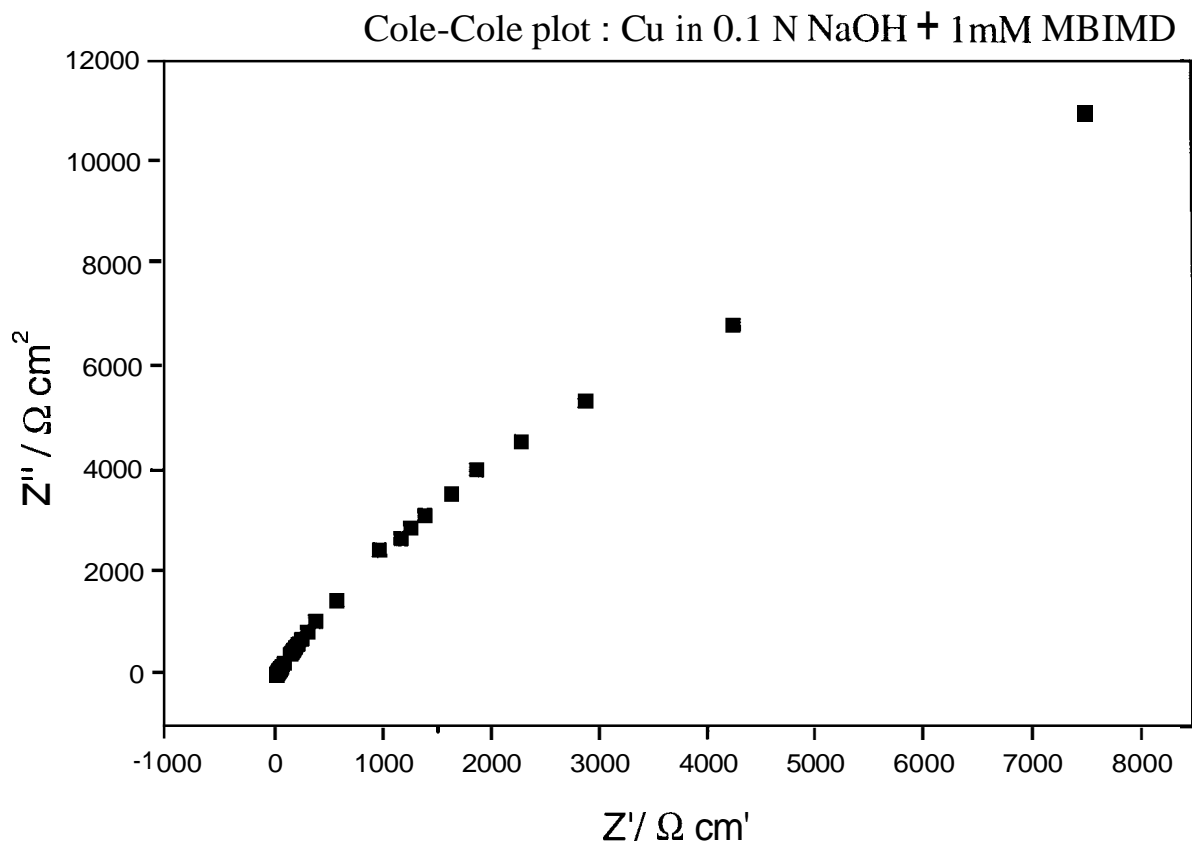
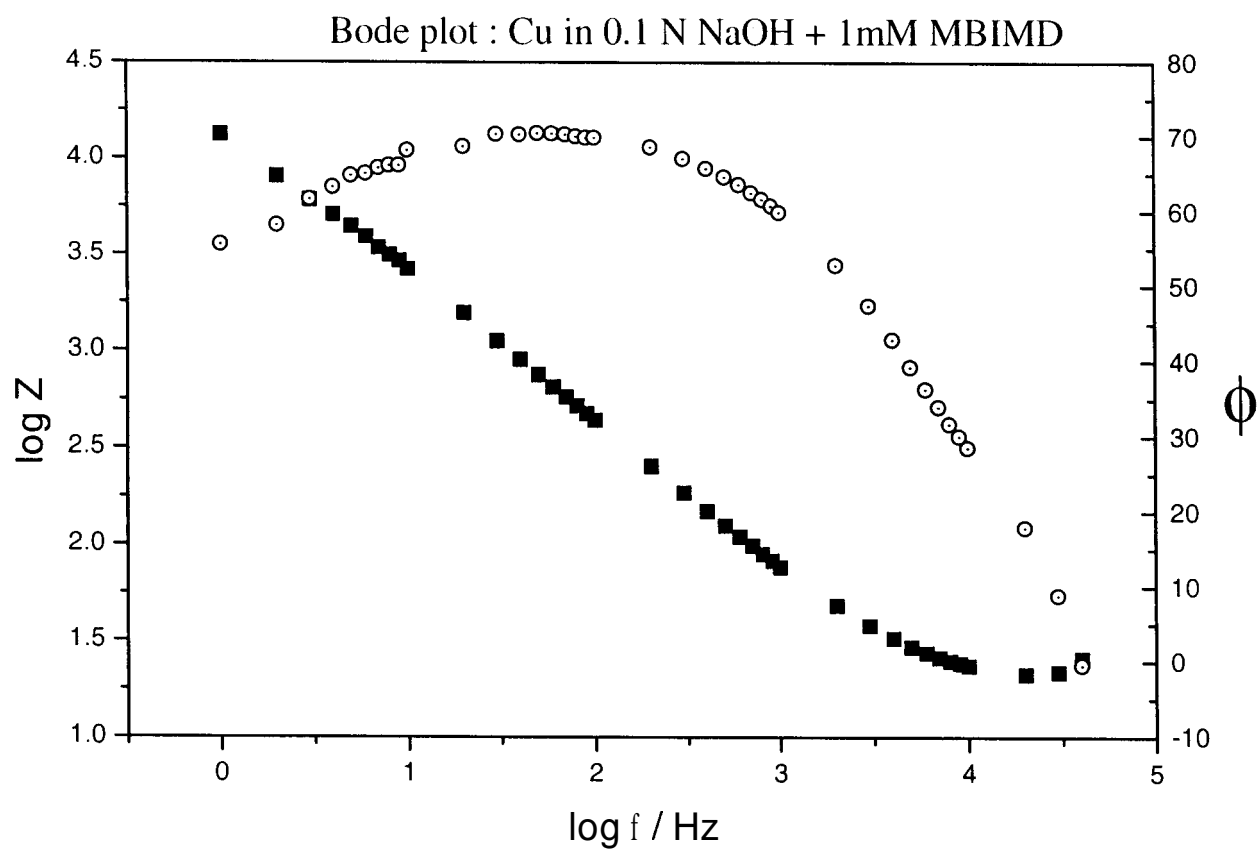
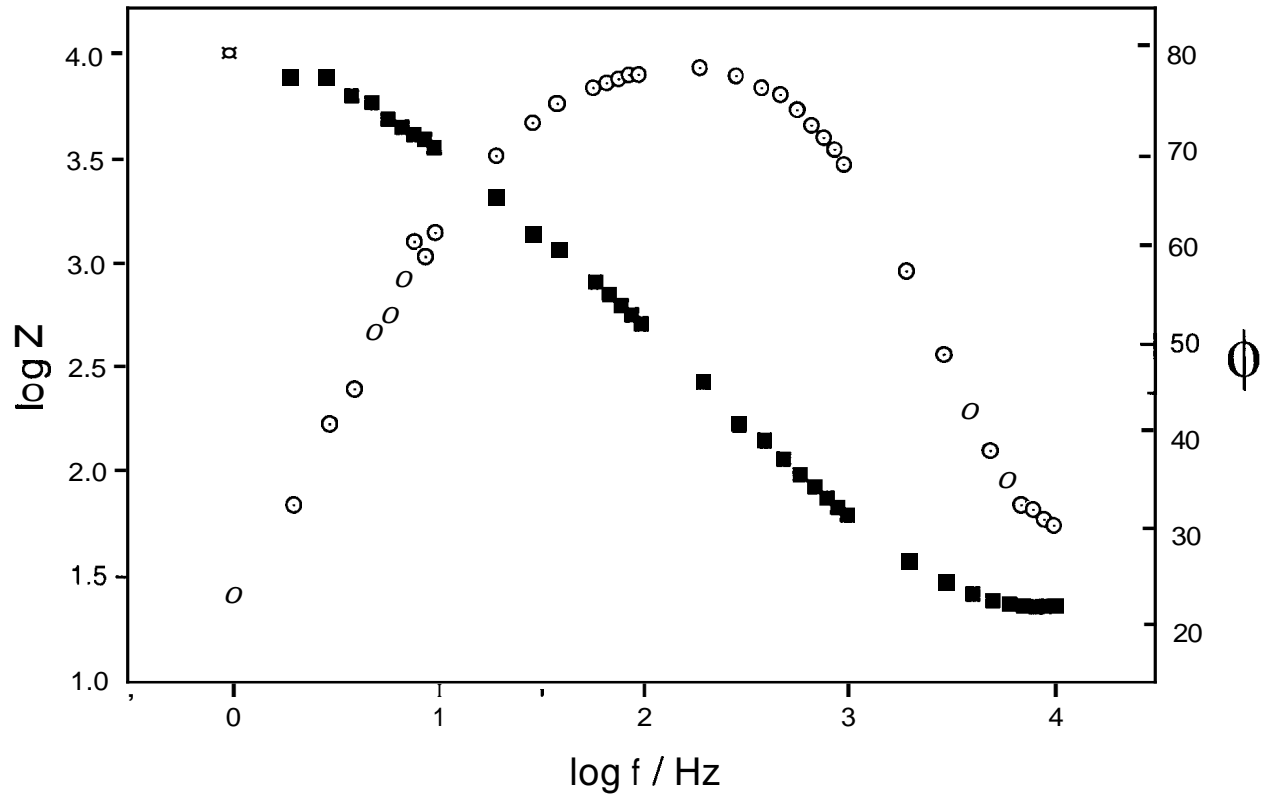


Figure - 13

Bode plot : Cu in 0.1 N NaOH + 1mM IMD



Cole-Cole plot : Cu in 0.1 N NaOH + 1mM IMD

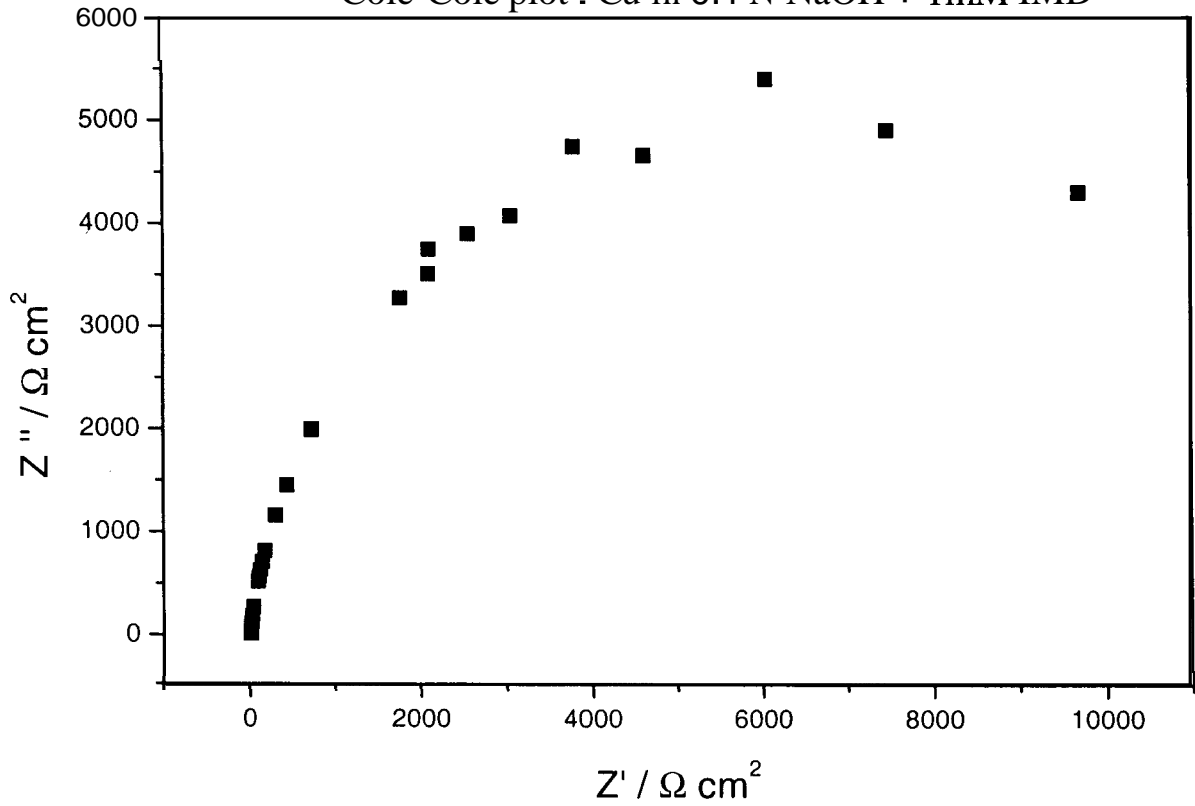


Figure - 14

Table 2

Double layer capacitance (C_{dl}) and charge transfer resistance (R_{ct}) of copper in the presence of different azoles in 0.1N NaOH

<i>COMPOUND</i>	R_{ct} (Ωcm^2)	C_{dl} ($\mu F cm^{-2}$)
<i>Blank</i>	258	13.7
<i>BTA</i>	14450	4.37
<i>MBT</i>	102500	1.763
<i>BIMD</i>	48000	0.961
<i>MBIMD</i>	51110	2.456
<i>IMD</i>	18474	3.538

We find that all the azoles decrease the double layer capacitance and increase the charge transfer resistance of the interface to different extents depending on the nature of adsorption. Greater the value of R_{ct} , better is the inhibiting power of the azole. This aspect is discussed later in this chapter.

- We observe that the entire impedance spectrum has only one time constant which is the result of a fast charge transfer process of copper dissolution.

3.6 Adsorption isotherms:

As discussed earlier the surface coverage θ of the electrode surface can be calculated from the charge under the cyclic voltammetric peaks using equation (2). The surface coverage θ for azoles at different values of inhibitor concentrations is shown in Table 3.

Table 3

Surface coverage (θ) for different azoles as a function of inhibitor concentration

<i>Concentration</i> (<i>mM</i>)	<i>BTA</i>	<i>MBT</i>	<i>BIMD</i>	<i>MBIMD</i>	<i>IMD</i>
0.1	0.11	0.27	0.17	0.23	0.17
0.2	0.26	0.49	0.50	0.36	0.25
0.5	0.45	0.62	0.74	0.49	0.35
0.7	0.52	0.76	0.77	0.56	0.39
1	0.57	0.84	0.79	0.68	0.43
2	0.64	0.89	0.82	0.74	0.46

We have tried to fit the coverage-concentration data to different adsorption isotherms [7]. We find that the inhibitor behaviour can be best fitted to the Langmuir adsorption isotherm. The Langmuir adsorption isotherm assumes that there is no interaction between the adsorbed species and that eventually surface saturation occurs.

The Langmuir adsorption isotherm (equation 5) can be rearranged as follows.

$$\frac{\theta}{1-\theta} = k c$$

$$\theta = k c - k c \theta$$

$$\theta(1 + k c) = k c$$

$$\theta = \frac{k c}{1 + k c}$$

$$\frac{c}{\theta} = \frac{1}{k} + c$$

Hence a plot of $\frac{c}{\theta}$ versus c should yield a straight line with intercept of $\frac{1}{k}$ if the inhibitor follows the Langmuir adsorption isotherm [11]. The adsorption isotherms obtained for different inhibitors are plotted in figures 15-19.

We find that while MBT, BIMD, MBIMD, show a good linear fit, there is a large deviation from linearity in the case of imidazole and to a lesser extent in the case of BTA. The equilibrium constant $k (M)^{-1}$ is calculated from the intercept from which the free energy of adsorption $\Delta G (kJ M^{-1})$ is obtained. The calculated values are tabulated in Table 4.

Table 4

Equilibrium constant (**k**) and free energy of adsorption (**AG**) for different azoles

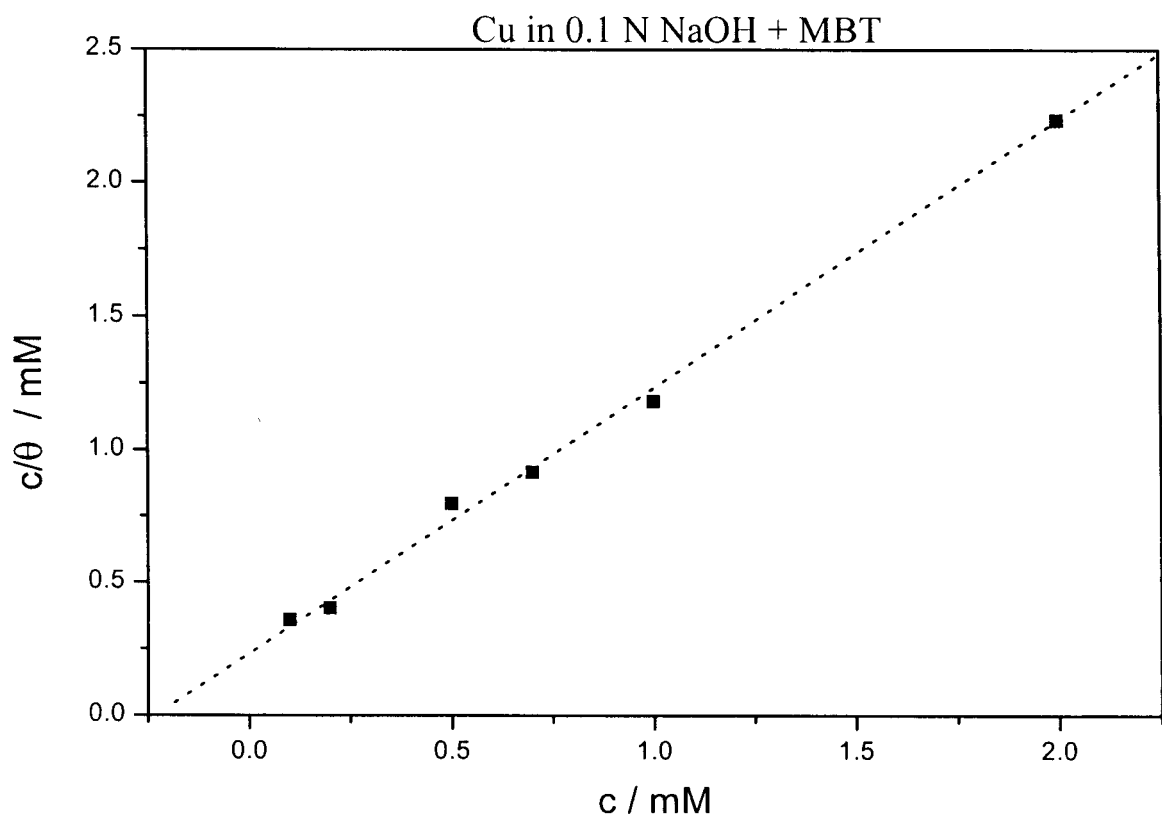
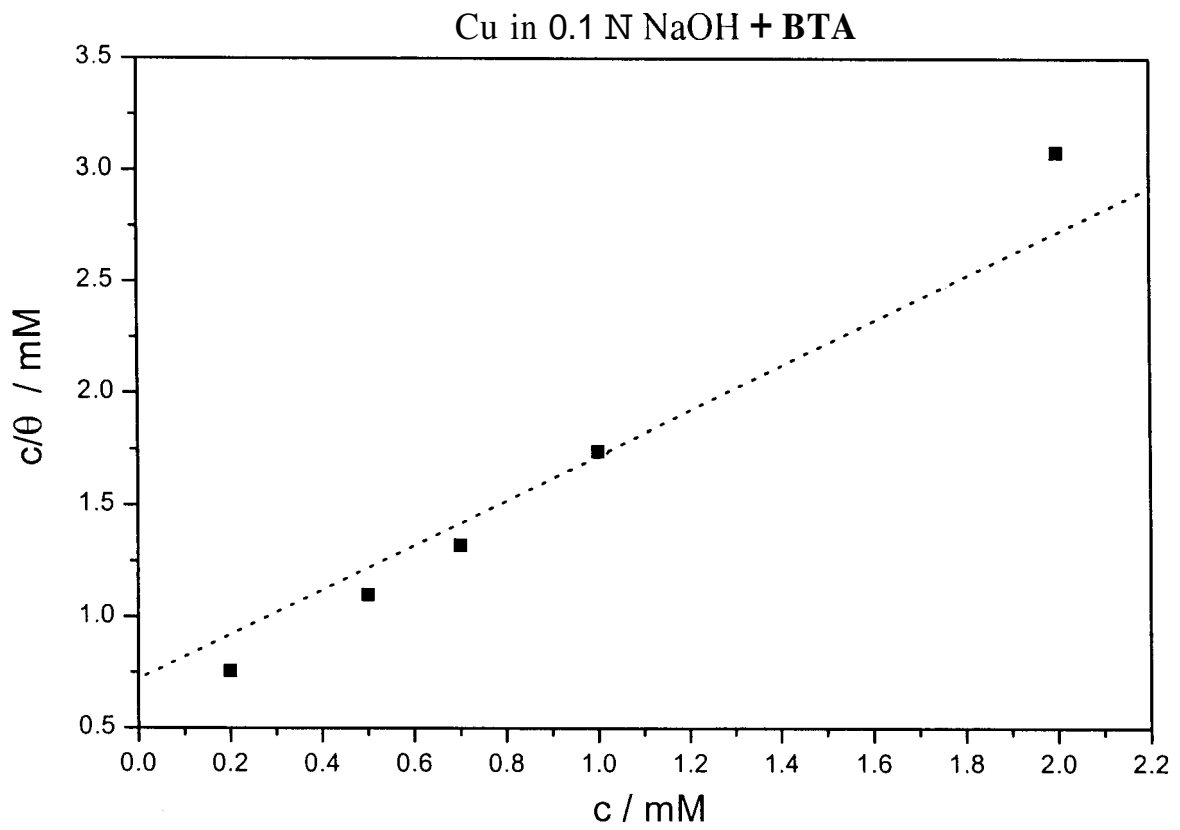
	BTA	MBT	BIMD	MBIMD	IMD
$k (M^{-1})$	1388.88	4347.82	4000	2127.65	900.9
$\Delta G (kJ M^{-1})$	-27.88	-30.71	-30.50	-28.94	-26.81

From Table 4 we find that MBT has the highest value of equilibrium constant and free energy of adsorption while IMD has the least value. Thus MBT has the largest tendency to react with copper.

3.7 Discussions and conclusions:

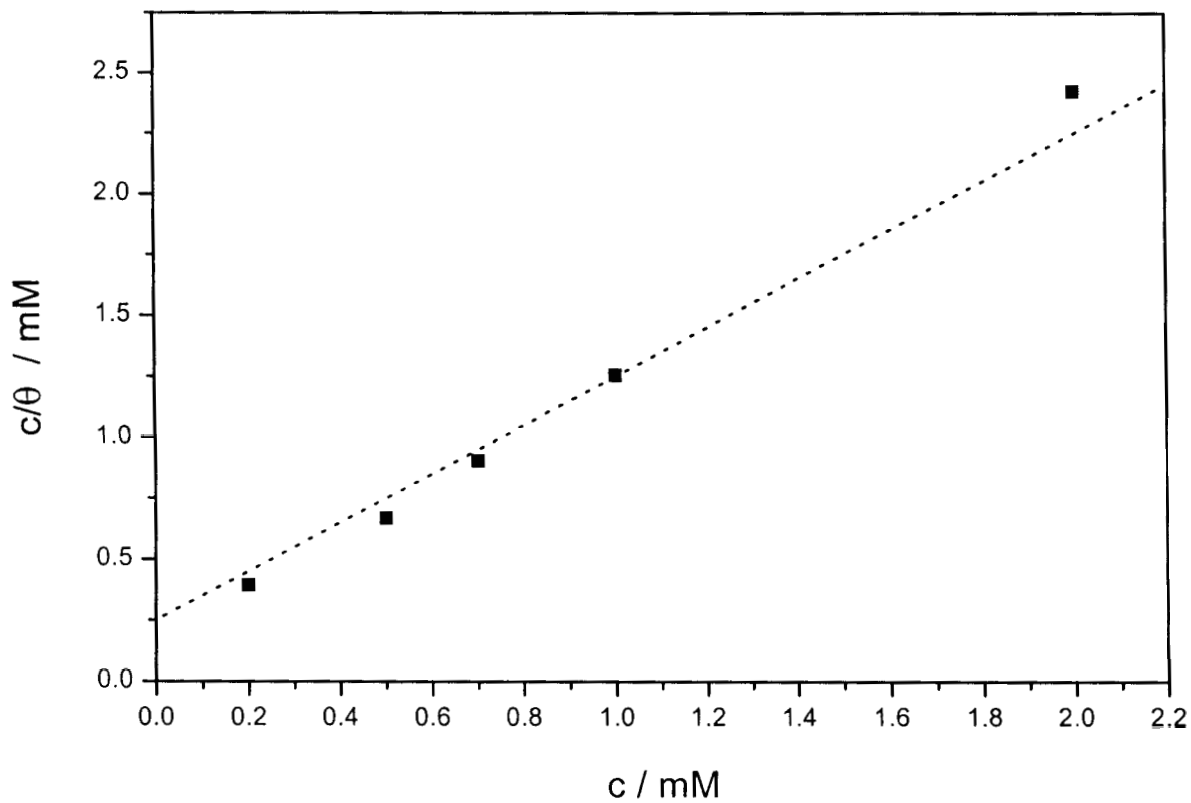
The cyclic voltammogram of Cu in 0.1 M NaOH shows the following peak potentials w.r.t $Hg/Hg_2SO_4, sat. Na_2SO_4$ reference electrode for the anodic and cathodic reactions.

1. $A_1 \rightarrow -0.8V$

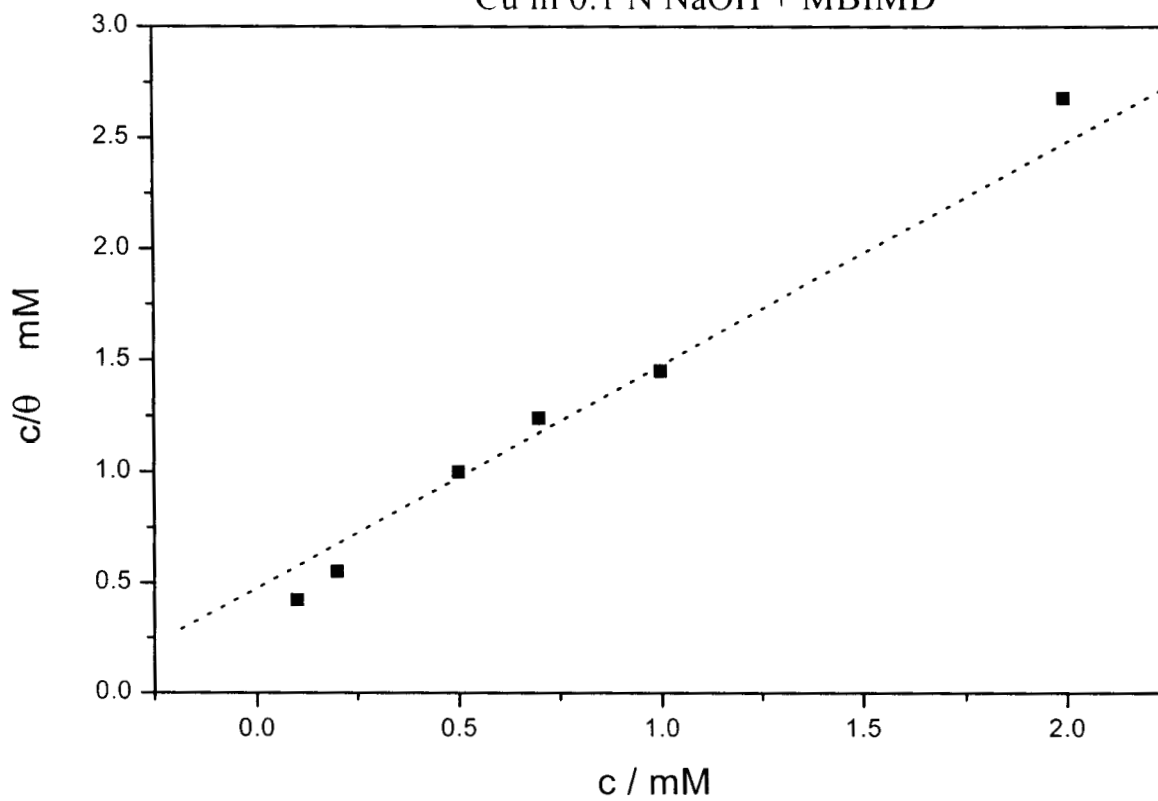


Figures 15 and 16

Cu in 0.1 N NaOH + BIMD



Cu in 0.1 N NaOH + MBIMD



Figures 17 and 18

Cu in 0.1 N NaOH + IMD

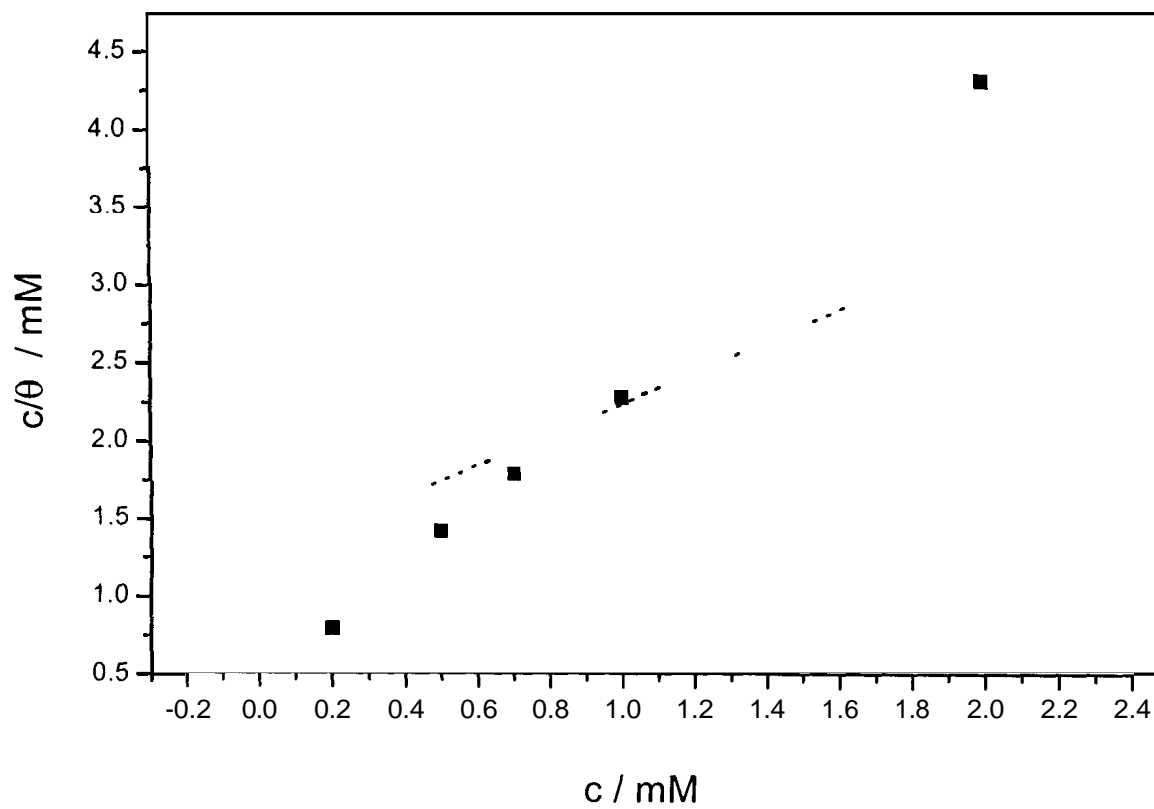


Figure - 19

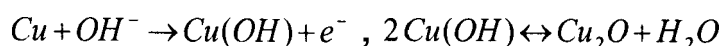
$$2. A_1 \rightarrow -0.53V$$

$$3. A_3 \rightarrow -0.4V$$

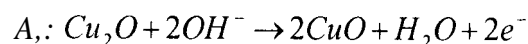
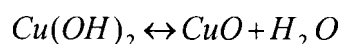
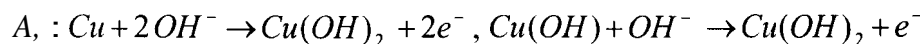
$$4. C_1 \rightarrow -0.87V$$

$$5. C_2 \rightarrow -1.2V$$

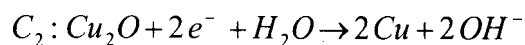
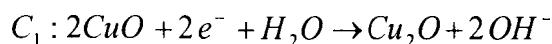
Peak A_1 is assigned to the electroformation of a Cu_2O layer.



whereas peaks A_3 and A_2 are associated with the anodic formation of a film of CuO that can proceed as follows.



The reduction scan shows two current peaks which are related to the electroreduction of CuO to Cu_2O and Cu_2O to Cu respectively.

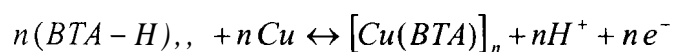


The presence of inhibitor at low concentrations does not cause significant changes in the potential ranges of the anodic and cathodic peaks but decreases the current density. By increasing the inhibitor concentration the anodic and cathodic peaks gradually diminish. There is also a displacement of the peak potentials at higher inhibitor concentrations.

3.7.1 Mechanism of inhibitor action:

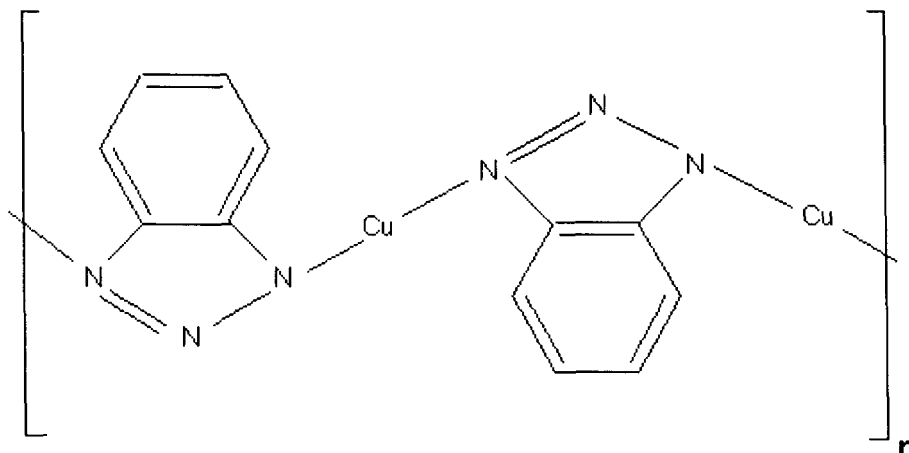
The efficiency of corrosion inhibitors is associated with chemical adsorption. The reaction mechanism includes the transfer of one pair of electrons from the organic compound and the formation of coordinate bonds with the metal. The inhibition efficiency strongly depends on the structure and chemical properties of the species formed under that particular experimental conditions. The extent of adsorption is dependent upon the electronic structure of the metal and the inhibitor, since chemisorption requires a chemical bond between the inhibitor and the metal. Benzotriazole (BTA) is a heterocyclic compound containing three Nitrogen atoms in the ring which is known to be an effective inhibitor for copper. Numerous surface analytical techniques have been employed to characterise the interaction between BTA and copper surface like ellipsometry, infra red reflection absorption spectroscopy (IRRAS), photo electron spectroscopy (XPS and AES) and Surface enhanced Raman spectroscopy (SERS)[12-15].

The copper electrode is always covered with a layer of copper oxide under ambient conditions. The Cu_2O layer provides a source of Cu^+ ions for BTA to react. Two types of mechanisms have been proposed for the inhibition of copper corrosion by BTA [15]. According to one mechanism BTA chemisorbs on the copper surface. The other is the formation of polymeric complexes with cupric ions. The polymeric complex can be overlaid with a layer of cupric oxide. The adsorption and complex formation are in equilibrium as follows:



which shows that increasing pH value and inhibitor concentration favours complex formation while chemisorption becomes more favoured in acid media and at low inhibitor concentration [16]. It can also be inferred from the above equation that the complex formation becomes less favourable if the potential changes to more negative values and vice versa. In alkaline medium BTA exists in the BTA^- form.

It reacts with copper and forms a thick polymeric film. The structure of the polymeric film [16] can be given as,



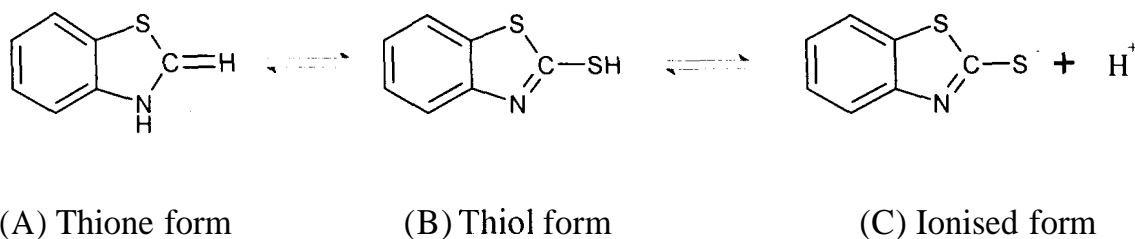
Structure of Cu-BTA polymeric film

The thickness of the polymer film is equivalent to many monolayers of $[Cu - (BTA)]$ monomers. The impedance spectrum of Cu in 0.1M NaOH in the presence of 1mM BTA gives a charge transfer resistance of $14460 \Omega cm^2$ as can be seen from figure 10 compared to the blank value of $258 \Omega cm^2$. This is possible if the electrode is covered with a thick polymeric film. The presence of the polymeric film also leads to a substantial reduction in the double layer capacitance C_{dl} of the interface which decreases from a value of $13.7 \mu F cm^{-2}$ for the bare electrode to $4.37 \mu F cm^{-2}$ as measured from the impedance plot (Table-2). This value is in reasonable agreement with the capacitance values obtained by Fox et al. [14] where they studied the variation of C_{dl} with potential of the copper surface covered with BTA in NaCl solution. The cyclic voltammetry of Cu in 0.1N NaOH in BTA also shows significant suppression of current at 1mM concentration. We find that the anodic peaks which correspond to the oxidation of copper are more drawn out compared with the blank. At a concentration of 1mM BTA we find that

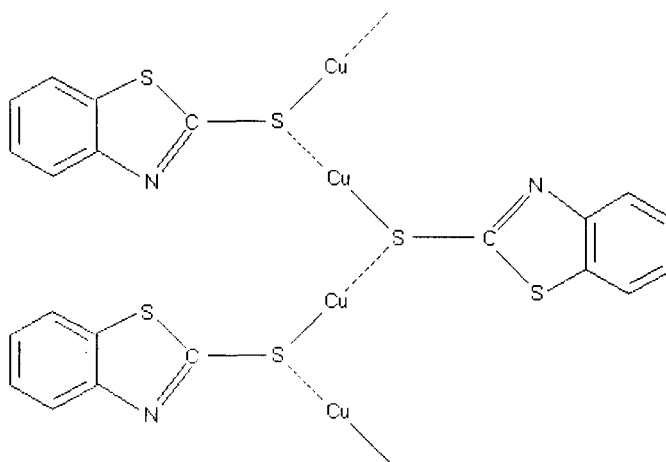
the second anodic peak is completely suppressed. With increasing concentration of BTA there is a progressive reduction in the anodic and cathodic peak currents. These processes may be due to the displacement of the solvent molecules coupled with the formation of the film. The protectiveness of the film is proportional to the degree of polymerisation. The buildup of a polymerised network of BTA-Cu chains is most strongly favoured on an oxidised Cu substrate. The different surface analytical techniques mentioned above have been used to elucidate a chain like structure for the BTA-Cu film at high pH values and concentrations. Ito et al. [13] have used polarisation-modulated infrared reflection absorption spectroscopy to study the surface films of BTA on copper. They find that the surface film is composed of infinite chains in which the Cu-BTA complex is connected by strong charge transfer interactions between the BTA molecules.

Mercaptobenzothiazole (MBT) has three atoms available for coordination i.e. N and S atoms in the ring and S atom of the thiocarbonyl group. The Sulphur atom of the thiazole ring is expected to have weak coordination ability since lone pairs on this atom participate in the resonating structure of the molecule, resulting in a reduction of electron density on the S atom and in a decrease of electron donating power.

Mercaptobenzothiazole exhibits the thiol-thione tautomerism [17] as:



In acidic solutions the thione form (A) is predominant, in basic solutions it is the ionised thiol form (C). We find the inhibitor efficiency of MBT to be the highest among all the azoles studied in this work. The double layer capacitance C_{dl} of the interface decreases from a value of $13.7 \mu F cm^{-2}$ for the bare electrode to $1.763 \mu F cm^{-2}$ as measured from the impedance plot (Table-2). The charge transfer resistance R_{ct} increases from a value of $258 S Z cm^2$ for the bare electrode to $102510 S Z cm^2$. This large increase suggests that MBT forms a very strong protective coating over the surface of copper preventing it from corrosion. The cyclic voltammogram of Cu in 0.1 N NaOH in the presence of 1mM MBT shows the almost complete suppression of both the anodic and cathodic peaks. Copper has a very high affinity towards sulphur. The S atom of the thiocarbonyl group (C = S) which is ionised in basic medium can react with copper to form a thick polymeric film. This conclusion is supported by the infra red and XPS studies on the Cu-MBT system by Ohsawa et.al.[17]. They find that a water insoluble polymeric film of mercaptobenzothiazolato – Cu(I) is formed on the surface by a surface reaction of cuprous ion with adsorbed MBT and that this film acts as a barrier against corrosive environments. The structure of the polymeric film based on these results can be proposed as,



A comparison of the inhibition properties of BTA and MBT indicates that MBT is a much better inhibitor of corrosion than BTA. Figure 20 shows a comparison between cyclic voltammograms of Cu in 0.1 N NaOH in the presence of 1mM BTA and MBT respectively. We can clearly observe MBT suppresses the anodic and cathodic peaks almost completely in contrast to BTA which shows partial suppression. This is also reflected in a larger value of charge transfer resistance and lower double layer capacitance of MBT over BTA. These observations suggest that MBT forms a more rigid, thicker and non permeable polymeric film compared to BTA.

Benzimidazole contains two nitrogen atoms in the five membered ring. Both the nitrogen atoms can coordinate with copper [18]. The R_{ct} value of Benzimidazole increases from 258Rcm^2 to 48000Rcm^2 as measured from its impedance spectrum. The C_{dl} value changes from $13.7\ \mu\text{F cm}^{-2}$ to $0.69\ \mu\text{F cm}^{-2}$. The cyclic voltammogram of Cu in the presence of 1mM Benzimidazole shows strong suppression of all the anodic and cathodic peaks.

Mercaptobenzimidazole (MBIMD) contains an additional sulphur group when compared with Benzimidazole. The R_{ct} value of MBIMD increases to a value of 51100Rcm^2 from the bare value while the double layer capacitance decreases to a value of $2.456\ \mu\text{F cm}^{-2}$. The cyclic voltammogram of MBIMD in the presence of inhibitor shows steep rise in anodic current towards the end of the forward scan possibly indicating instability of the film at more positive potentials.

Imidazole is a heterocyclic organic compound with three carbon and two nitrogen atoms in the ring. The imidazole molecule shows three different anchoring sites suitable for surface bonding: the nitrogen atom with its lone sp^2 electron pair, the edge carbon atoms and the aromatic ring [19]. We find from cyclic voltammetry that imidazole has the least inhibiting effect towards copper corrosion compared to the other inhibitors. However from the impedance spectrum we find that the R_{ct} value is marginally greater than that of BTA. The double layer

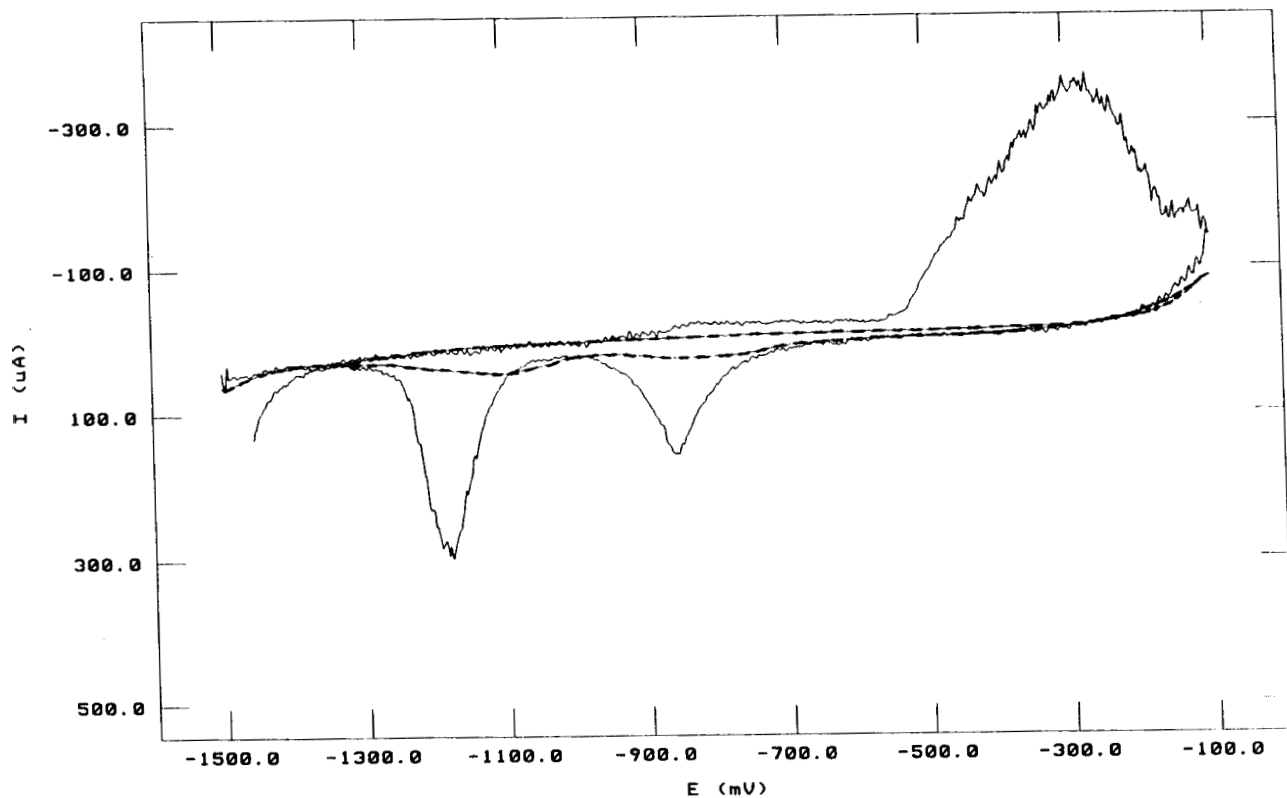


Fig 20 : Comparison of CVs of copper in 0.1M NaOH with the addition of 1mM BTA and 1mM MBT. Scan Rate : 20 mV /s

———— with BTA

- - - - - with MBT

capacitance upon adsorption is found to be $3.538 \mu F cm^{-2}$ which is also lower than that of BTA. Xu et al. [20] observe that di-imidazolato copper (II) complex is formed by the reaction of metallic copper with imidazole. Di-imidazolato copper is insoluble in common solvents and is polymeric in nature.

Benzimidazole has the lowest value of C_{dl} compared to all the other azoles studied. However its R_{ct} value is lower than that of MBT. This suggests that it forms a thicker polymeric film compared to the other azoles. The polymeric film formed however might be more permeable to solvent molecules and copper ions than films formed by MBT and BIMD resulting in higher corrosion rate. BIMD and MBIMD have the same structure except for the additional $-SH$ group in MBIMD. A comparison of the cyclic voltammetric curves of BIMD and MBIMD (figure 21) at 1mM concentration shows that BIMD has better inhibition than MBIMD towards copper dissolution.

Tetrazole does not have any effect on the corrosion of copper in 0.1 M NaOH solution. The cyclic voltammetric peaks of copper in 0.1 M NaOH in the presence of 1mM Tetrazole show no perceptible blocking behaviour (figure 9).

We can obtain a relative comparison of the inhibition power of the different azoles studied from the values of charge transfer resistance, double layer capacitance, equilibrium constant and free energy values measured. Based on these results the inhibition efficiency of the different azoles towards corrosion of copper in 0.1 N NaOH solution can be placed in the following order:

$$MBT > BIMD \approx MBIMD > BTA \approx IMD$$

McCrorry-joy et al.[18] have carried out cyclic voltammetry and chronocoulometric studies to study the inhibitor effect of BTA, BIMD and IMD on copper in acetate buffered media at pH 3, 4.5 and 6. They find that BTA has the best inhibition efficiency among the three azoles followed by BIMD and IMD. We

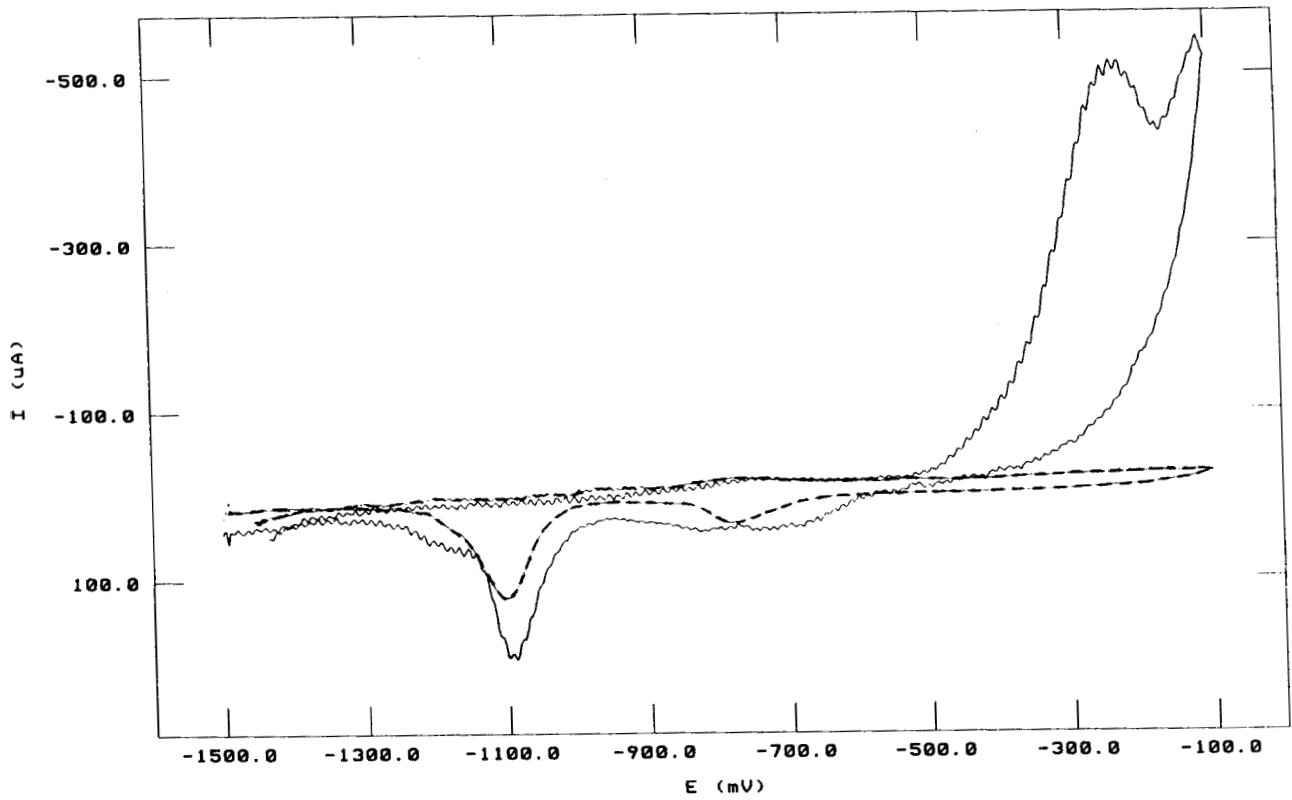


Fig 21 : Comparison of CVs of copper in 0.1M NaOH with the addition of 1mM Benzimidazole and 1mM Mercaptobenzimidazole . Scan Rate : 20 mV /s

————— with MBIMD - - - - - with BIMD

find that BIMD has better inhibition efficiency than BTA and IMD towards inhibition of copper corrosion in 0.1 N NaOH.

From the above results and that of ours we can conclude that the inhibition efficiency of a particular inhibitor depends on the pH of the solution. A compound which has a relatively poor inhibitive effect at a particular pH can behave as a good inhibitor for the same metal at a different pH.

It can also be observed that the azoles which show relatively less inhibition like Imidazole (IMD) and no inhibiting characteristics like Tetrazole (TTA) do not contain an aromatic ring. The presence of the aromatic ring might help cover a greater area of the electrode surface if the ring lies parallel to the electrode surface. The π electron cloud of the benzene ring can also overlap with the vacant d-orbitals of copper facilitating effective adsorption and thereby screening the electrode from the solution.

REFERENCES

1. M.G.Fontana and R.W.Staehle (Edited) Volume 1 *Advances in corrosion science and technology* Plenum Press New York – London 1970.
2. A.D.Modestov, G.D.Zhou, Y.P.Wu, T.Notoya, D.P.Schweinsberg *Corrosion Science* Vol.36, No.11, (1994), 1931-1946.
3. R..M.Souto, V.Fox, M.M.Laz, M.Perez, S.Gonzalez *J.Electroanal. Chem.* 411, (1996), 161-165
4. Richard R.Thomas, V.A.Brusic, B.M.Rush *Journal of the Electrochemical Society* Vol.139, No.3 March 1992.
5. E.Stupnisek-Lisac, A.Loncaric Bozic, I.Cafuk *Corrosion* Vol.54 No.9 (1998) 713-720.
6. R.Babic, M.Metikos-Hukovic, M.Loncar *Electrochimica Acta* 44 (1999) 2413-2421.
7. B.B.Damaskin, O.A.Petrii and V.V.Batratkov *Adsorption of organic compounds on electrodes.* Plenum Press, New York – London (1971).
8. S.M.Abd El Haleem, B.G.Ateya *J.Electroanal. Chem.*, 117 (1981) 309-319.
9. *Instrumental Methods in Electrochemistry.* Southampton Electrochemistry group. Ellis Horwood Limited (1990). pg. 268.
10. Christopher M.A.Brett and Anna Maria Oliveira Brett *Electrochemistry Principles, Methods and Applications* Oxford University Press 1993. pg.234
11. A.A.Taha, A.M.Ahmed *Bulletin of Electrochemistry* 10, (2-3), Feb – Mar 1994, 136 - 141
12. M.Fleischmann, I.R.Hill, G.Mengoli, M.M.Musiani, J.Akhavan *Electrochimica Acta* Vol.30, No.7 (1985) 879-888.
13. M.Ito, M.Takahashi *Surface Science* 158 (1985) 609-615.
14. P.G.Fox, G.Lewis, P.J.Boden *Corrosion Science* Vol.19, (1979) 457-467.
15. Zhi Xu, Sharon Lau, P.W.Bohn *Langmuir* 9 (1993) 993-1000

16. K.Aramaki, T.Kiuchi, T.Sumiyoshi, H.Nishihara *Corrosion Science* Vol.32, No.5/6, (1991), 593-607.
17. M.Ohsawa, W.Suetaka. *Corrosion Science* Vol.19, (1979), 709-722.
18. C.McCrory-Joy, J.M.Rosamilia *J. Electroanal Chem.* 136(1982) 105-118.
19. E.Stupnisek-Lisac, A.Loncaric Bozic, I.Cafuk *Corrosion* Vol.54 No.9 (1998) 713-720.
20. G.Xue, S.Jiang, X.Huang, G.Shi, *J.Chem. Soc. Dalton Trans.* (1988) 1487.